Arabian Journal of Chemical and Environmental Research

Vol. 11 Issue 2 (2024) 137–160

Green Synthesis and Antimalarial Assessment of Hydrazone-Based Metal Complexes: A Non-solvent Approach for the Discovery of New Drugs

***S. T. Dafa[1], U.J. Ahile[2], M. S. Iorungwa[3], R. A. Wuana[3], E. N. Iornumbe[3], I. T. Iorkpiligh[2], E. Tanko[1] and E. D. Terungwa[1]**

[1]*Department of Chemistry, Federal University of Technology Minna, Niger State*
[2]*Department of Chemistry, Benue State University, Makurdi, Nigeria*
[3]*Inorganic/Physical Chemistry Research Group, Department of Chemistry, Joseph Sarwuan, Tarka University, Makurdi, Nigeria*

Corresponding Author: dafaterungwa@futminna.edu.ng
Co-authors emails: ahileuj@gmail.com; savior.moses@gmail.com; raywuana@yahoo.com; estnguior@gmail.com; mynameisterungwa@gmail.com; ezekieltanko@gmail.com; agaelizabeth35@gmail.com

Received 13 Nov 2024, Revised 23 Dec 2024, Accepted 27 Dec 2024

Cited as: *Dafa S. T., Ahile U.J., Iorungwa M. S., Wuana R. A., Iornumbe E. N., Iorkpiligh I. T., Tanko E. and Terungwa E. D. (2024) Green Synthesis and Antimalarial Assessment of Hydrazone-Based Metal Complexes: A Non-solvent Approach for the Discovery of New Drugs, Arab. J. Chem. Environ. Res. 11(2), 137-160*

Abstract

The rise of drug-resistant *Plasmodium* strains has increased the worldwide need for potent and eco-friendly antimalarial treatments. This study meets that need by presenting a method to synthesise hydrazone-based metal complexes without solvents, a promising but rarely used approach in developing antimalarial drugs. In this study, (E)-4-[(2,4-dinitrophenyl) hydrazonomethyl] phenol (**L_1**) and N-(4-hydroxybenzaldehyde)-p-fluoroaniline (**L_2**) were synthesised alongside their complexes utilising grinding as a non-solvent method. The compounds were characterised by molar conductance, solubility, melting point, UV-Vis, and FTIR. Surface morphologies were analysed through SEM, and the particle sizes were measured at a diffraction angle of 10.9°. The freshly synthesised compounds were tested for their antimalarial activities. The synthesised compounds showed stability and non-electrolytic behaviour, with molar conductance values of 5.5 - 16.20 Ω/cm^{-2}. FTIR spectra showed bidentate ligands coordinated via azomethine and hydroxyl groups, while UV-Vis results displayed bathochromic shifts on complexation, indicating successful chelation with metal ions. The differences in the morphologies of the ligands and their complexes generated by SEM images suggest coordination during grinding. The antimalarial study showed increased activity with concentration increase and species-dependent efficacy, as it was more effective against *Culex quinquefasciatus* eggs than *Anopheles gambiae*. This study illustrates the potential of hydrazone-based metal complexes synthesised through a solvent-free, environmentally friendly method as candidates for novel antimalarial treatments.

Keywords: Green synthesis, Non-solvent, (E)-4-[(2,4-dinitrophenyl) hydrazonomethyl] phenol, N-(4-hydroxybenzaldehyde)-p-fluoroaniline, *Culex quinquefasciatus* and *Anopheles gambiae*

*Corresponding author. *E-mail address:dafaterungwa@futminna.edu.ng*

1. Introduction

Malaria is one of the leading causes of mortality worldwide, mainly affecting sub-Saharan Africa, as well as parts of Asia and Latin America (Oladipo *et al.*, 2023). The rise and spread of drug-resistant strains of *Plasmodium species*, the pathogens responsible for malaria, provide a substantial public health challenge, despite notable advancements in their management and treatment (Massand *et al.*, 2013; Plowe, 2022; Segovia *et al.*, 2025). Resistance to essential antimalarial medications, including chloroquine, sulfadoxine, pyrimethamine, and artemisinin-based combination treatments (ACTs), has been progressively documented, threatening the advancements made in the last twenty years. This growing dilemma highlights the pressing need for innovative, efficacious, and ecologically sustainable antimalarial medicines (White, 2019; WHO, 2024).

In light of this challenge, metal-based pharmaceuticals and coordination complexes have reaped substantial interest in therapeutic chemistry owing to their structural diversity, distinctive reactivity, and mechanisms of action that differ from traditional organic drugs (Jalal *et al.*, 2020; Kapusterynska *et al.*, 2023; Wang *et al.*, 2024; Rai *et al.*, 2011). Hydrazone-based metal complexes are notable for their extensive array of biological activities, encompassing antibacterial, anticancer, and antiparasitic effects (Sharma *et al.*, 2020; Liu *et al.*, 2022; Sarıoğlu *et al.*, 2024). They are also excellent inhibitors of metal corrosion in acidic media (Khamaysa *et al.*, 2020; Chaouiki *et al.*, 2020; El-Khlifi *et al.*, 2024). Hydrazones include adaptable donor atoms that efficiently coordinate with transition metals, henceforth improving the stability and bioactivity of the produced complexes (Shakdofa *et al.*, 2014; Salah *et al.*, 2019; Brum *et al.*, 2020).

Conventional synthesis procedures for these metal complexes often depend on organic solvents, many of which pose dangers to humans and the environment. These behaviours result in the development of chemical waste, elevated energy consumption, and probable toxicity (Kharissova *et al.*, 2019; López-Lorent *et al.*, 2022). In line with the principles of green chemistry, there is a growing interest in creating more sustainable alternatives (Alshahateet *et al.*, 2024a & 2024b; Titi *et al.*, 2020a & 2020b). A notable method is non-solvent synthesis, which omits hazardous solvents, thereby reducing environmental effects and improving safety (Barbara, 2020; Dafa *et al.*, 2023).

Although there is an expanding amount of research on hydrazine-based complexes and their biological attributes, few studies have explored their synthesis through non-solvent methods, especially concerning the structural characterisation and antimalarial studies of hydrazone-metal complexes containing Co(II), Mn(II), and Ni(II). This research fills the gap by utilising grinding as a non-solvent synthetic method to synthesise and characterise Co(II), Mn(II), and Ni(II) hydrazone-based metal complexes. It further studies their antimalarial properties, aiming to further the growth of environmentally sustainable, metal-based treatments to address the ongoing and evolving challenge of malaria.

2 Materials and methods

The study utilised 4-hydroxybenzaldehyde, 2,4-dinitrophenylhydrazine, and 4-fluoroaniline (all sourced from BDH, UK) to synthesise the ligands, which were subsequently complexed with hydrated Co(II), Mn(II), and Ni(II) chlorides. Solubility studies were performed utilising methanol, diethyl ether, petroleum ether, DMSO, DMF, and acetone (May and Baker, Nigeria), with DMSO and acetone further employed as solvents for antimalarial testing formulations. A multitude of instruments were utilised, comprising a Barnstead BI9100 electrothermal apparatus for melting point assessment, an Accumet AP75 conductivity meter, a Rigaku D/Max-lllC X-ray diffractometer, a JSM 7600F scanning electron

microscope, a Perkin Elmer 3000 MX spectrometer, and an OV/100/F oven for weighing and drying synthesised compounds.

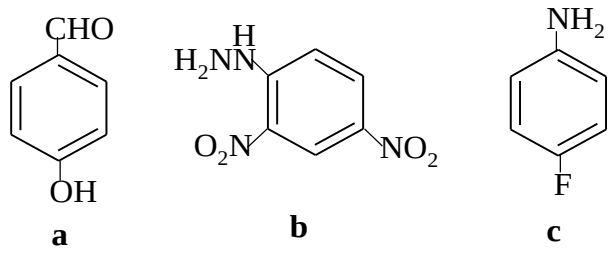

Scheme 1: Important Precursors Involved in Ligand Synthesis, Structures of 4-Hydroxybenzaldehyde (**1a**), 2,4-Dinitrophenylhydrazine (**1b**), and 4-Fluoroaniline (**1c**)

2.2 Green synthesis of (E)-4-[(2,4-dinitrophenyl)hydrazonomethyl]phenol (L_1): A vital ligand for metal complex formation

The green synthesis of E-4-[(2,4-dinitrophenyl)hydrazonomethyl]phenol (L_1) was carried out using the method reported by El-Barasi *et al*. (2020), but with notable modifications. 4-hydroxybenzaldehyde (0.01 mol) and 2,4-dinitrophenylhydrazine (0.01 mol) were grinded together in a porcelain mortar for 10 min, yielding 95 % of an orange-coloured microcrystalline compound as shown in equation 1.

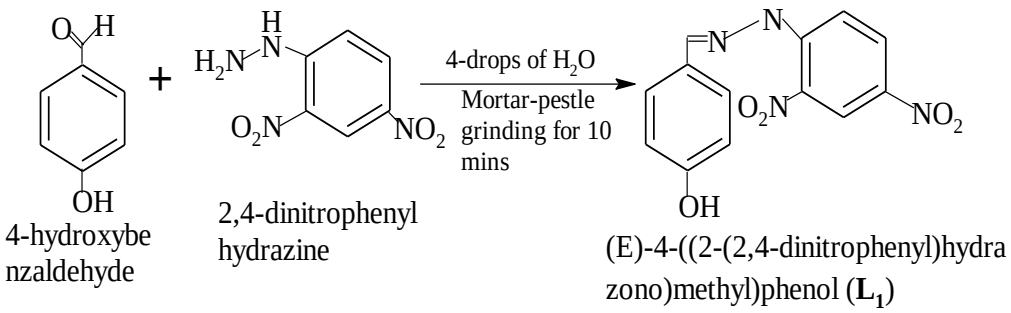

(1)

2.3 Green synthesis of N-(4-hydroxybenzaldehyde)-p-fluoroaniline (L_2)

N-(4-Hydroxybenzaldehyde)-p-fluoroaniline (**L_2**) was synthesised following the procedure established by Ommenya *et al*. (2020), with minor adjustments. Specifically, 4-fluoroaniline (0.00319 mol) was mixed with 4-hydroxybenzaldehyde (0.00319 mol) and ground in a mortar with a pestle for 10 min, resulting in an immediate thick yellow-orange product. The product was subsequently dried in an oven at 70 °C, producing lustrous, needle-like, yellow-orange crystals.

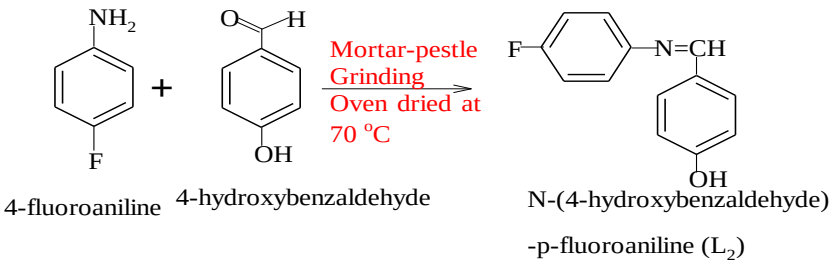

(2)

2.4 Green Synthesis of the metal(II) complexes with Hydrazone Ligand

Metal(II) hydrazone-based complexes were synthesised through the mixing of the ligands (0.01 mol of L_1 and L_2) with the metal(II) salt [0.01 mol of Co(II), Mn(II), and Ni(II) salts] as described by Ommenya

et al. (2020) and grinding in a mortar with pestle for 10 min. The resulting product was oven-dried at 70 °C, yielding 96, 97, and 95 % of coloured microcrystalline Co(II), Mn(II), and Ni(II) complexes.

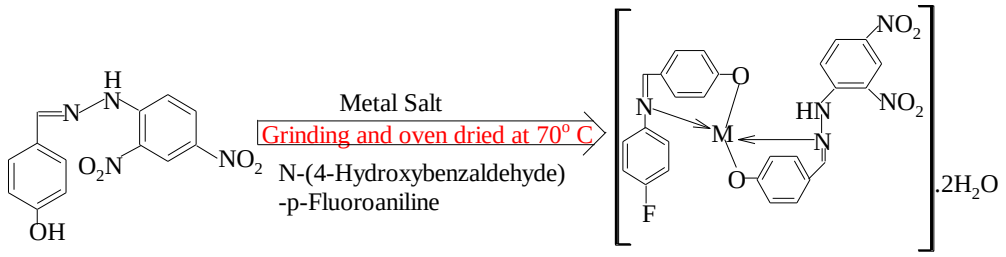

(3)

2.5 Characterization of the synthesized ligands and their complexes

2.5.1 Solubility tests

The solubility test was carried out as reported by Iorungwa *et al*. (2019). In separate test tubes containing methanol, ethanol, dimethylformamide, dimethylsulfoxide, distilled water, and acetone, 0.01 g of the synthesised ligands and complexes were rapidly shaken with 10 mL of solvent. The sample was classed as soluble (**X**) if, after shaking, the whole solute dissolved, resulting in a homogenous mixture. However, the sample was classified as slightly soluble (**Z**) if some of it dissolved while others remained, and insoluble (**Y**) if the solute remained as it was introduced.

2.5.2 Melting point determination

A sample of each synthesised compound was placed in a separate capillary tube to a depth of 2 mm, with the bottom tapped multiple times to ensure close packing. The tubes were then inserted into a heating block and heated, and the melting point of each sample was recorded from the digital display. This process was repeated for all samples (Iorungwa *et al*., 2019).

2.5.3 Conductivity measurement

Conductivity measurement was carried out as described by Martínez (2018) and Zou *et al*. (2019) by weighing exactly 10 g of air-dry soil (less than 2 mm) into a bottle, adding 50 mL of deionised water using an Accumet AP75 meter, and shaking the mixture mechanically for one hour at 15 rpm to dissolve soluble salts, resulting in a 1:5 soil water suspension. The cell was properly cleaned after the conductivity meter was calibrated using the KCl reference solution, following the manufacturer's instructions to determine the cell constant. Without moving the settled soil, the conductivity cell was filled with ligands and their complexes after being washed with the soil suspension. The temperature of the soil suspension and its electrical conductivity of 0.01M KCl were found at the same time. We noted the conductivity values of ligands and their complexes based on what the conductivity meter showed.

2.5.4 Infrared and electronic spectra studies

The synthesised ligands and their complexes were run as KBr discs and shown on the Perkin Elmer 3000 MX FT-IR spectrophotometer spectrum BX with spectrum version 5.3.1 software version. All spectra were acquired from 4000 to 400 cm^{-1} using the PerkinElmer 3000 MX spectrometer, and the IR spectra were analysed using the spectroscopic program Win-IR Pro Version 3.0 with a peak sensitivity of 2 cm^{-1}. The UV spectra of the produced complexes were obtained using acetone as solvent from a Perkin Elmer UVD-2690 UV-VIS double beam PC scanning spectrophotometer (UV-Winlab 2.8.5.04) software version (Luo, 2014).

2.6 Preparation of varying concentrations of L_1, L_2, and their Co(II), Mn(II) and Ni(II) complexes

Multiple concentrations of the synthesised ligands and metal complexes were prepared using the method of Iorungwa *et al*. (2020). A 100 mg/mL solution of 10 % dimethyl sulfoxide (DMSO) was used to dissolve 1.0 g of the L_1, L_2, Co(II), Mn(II), and Ni(II) complexes. To obtain a concentration of 500 mg/mL, the stock solution was diluted in acetone by mixing 10 mL of the stock solution with 10 mL of acetone and shaking vigorously. Dilutions of 250, 125, and 62.5 mg/L were subsequently prepared by mixing 5 mL of the 500 mg/mL solution with 5 mL of acetone.

2.7 Field Collection and Laboratory Rearing of Mosquito Larvae for Species Identification

Mosquito larvae were collected from stagnant water using plastic dippers and sieves as described by Atabo *et al.* (2019). They were reared in a netted cage in a closed system at the Entomology Research laboratory of the Zoology Department, Joseph Sarwuan University, Makurdi. The larvae were identified as *Anopheles gambiae* and *Culex quinquefasciatus*. They metamorphosed into adult mosquitoes, which were then aspirated into a new cage with skin-scrapped Guinea pigs for a blood meal and egg development. A glucose solution was added for energy and egg laying. Fish meal was fed until the third and fourth instar of the second filial generation larvae were obtained (Araújo *et al*., 2012; Ong and Jaal, 2018; Zanin *et al*., 2019).

2.8 Assessment of Egg and Larvae Mortality induced by Synthesized Compounds

The egg and larvae mortality induced by the synthesised ligands and complexes was assessed using the existing methods of Munusamy *et al.* (2016) and WHO (2016), with slight changes. Various concentrations of 62.5, 125, 250, and 500 mg/L diluted in acetone were tested on *Anopheles gambiae* and *Culex quinquefasciatus* eggs that had just been laid and early third-instar larvae. This was repeated multiple times for each test. Azadirachtin (10.0 mg/L) functioned as a positive control, and independent controls were further performed. Egg hatchability (Ovicidal activities) and larval mortality (Larvicidal activities) were evaluated after 24 hrs. Non-hatching eggs and larvae that failed to reach the surface were classified as dead using the formulas below.

$$\%\ \text{Mortality of Mosquito's Eggs} = \frac{\text{Number of unhatched eggs}}{\text{Total number of eggs introduced}} \times 100 \quad (4)$$

$$\%\ \text{Mortality of Mosquito's Larvae} = \frac{\text{Number of dead Larvae}}{\text{Total number of Larvae introduced}} \times 100 \quad (5)$$

3. Results and Discussion

3.1 Physical Properties Results

Crystalline and coloured metal complexes were formed by the interaction between the synthesised ligands, $\mathbf{L_1}$ and $\mathbf{L_2}$, and the Co(II), Mn(II), and Ni(II) ions. Since none of the final colours of the products matched those of the starting ingredients, it was evident that reactions had occurred during the synthetic step. The ligands and their complexes melted between 188 and 194 ℃ , suggesting they were relatively stable compounds. Conversely, their conductance values extended from 5.2 to 16.20 $Ohm^{-1}\cdot m^{-1}$ (Table 1), which was less than 50 $Ohm^{-1}\cdot m^{-1}$, signifying that they were non-ionic (Ommenya *et al*., 2020). Since conductivity is a physical property used to classify ligands alongside complexes as electrolytes and non-electrolytes based on their values, this validates that no anions existed outside the coordination sphere of the complexes (Pavčnik *et al*., 2024). The information obtained from the conductivity test can be invaluable in determining the structure of the complexes because it introduces primary and secondary

valence, which Werner used to support his theory (Heinz, 2014). The ligands and their complexes were observed to be non-soluble in water, however, they exhibited minor solubility or solubility in other common organic solvents such as acetone, dimethyl sulfoxide (D.M.S.O.), dimethylformamide (D.M.F.), and petroleum ether. The solubility of ligands and their complexes is a crucial characteristic that reflects their polarity, sets them apart from other substances, and informs their applications. The fact that the ligands and complexes do not dissolve in water shows that they are nonpolar (Heuer-Jungerman *et al*., 2019). This is because they have covalent and coordinate covalent bonds, demonstrating there are no ionic bonds to help them dissolve in water (Anand *et al*., 2022). The insoluble status of the complexes in water excludes the presence of counter ions in the complexes or the existence of charged complexes (Andriianova *et al*., 2020). The solubility of the ligands and their complexes increased in polar solvents: methanol, ethanol, acetone, and DMSO, resulting in modest solubility in methanol and ethanol and full solubility in acetone, DMF, DMSO, and petroleum ether. The improvement in solubility can be attributed to the presence of substituents (-OH, -F, -NO_2) placed at the ortho and para positions of the aromatic ring. These substituents may enhance solubility in both organic and inorganic solvents (Sittel *et al*., 2021; Das *et al*., 2022).

Table 1: Physical Properties of Synthesised Ligands with their Complexes

Compound	Colour	Melting Point (°C)	Conductivity (Ohm $^{-1}$m^{-1})
L_1	Red pink crystals	190.00	5.50
L_2	Brown crystals	194.00	5.80
Co(II)L_1	Pink crystals	184.00	5.10
Mn(II)L_1	Pink crystals	186.00	5.30
Ni(II)L_1	Orange crystals	187.00	5.40
Co(II)L_2	Light blue crystals	190.00	5.60
Mn(II)L_2	Dark brown	191.00	5.70
Ni(II)L_2	Gray crystals	192.00	6.20
Co(II) L_1L_2	Black crystals	185.00	5.20
Mn(II) L_1L_2	Reddish brown crystals	188.00	6.20
Ni(II) L_1L_2	Pink crystals	191.00	16.20

Table 2: Solubility Profile of Ligands and their Metal Complexes at Room Temperature

Compounds	Distilled Water	Methanol	Ethanol	D.M.F	Acetone	D.M.S.O	Petroleum ether
L_1	Y	Z	Z	X	X	X	X
L_2	Y	Z	Z	X	X	X	X
Co(II)L_1	Y	Z	Z	X	X	X	X
Mn(II)L_1	Y	Z	Z	X	X	X	X
Ni(II)L_1	Y	Z	Z	X	X	X	X
Co(II)L_2	Y	Z	Z	X	X	X	X
Mn(II)L_2	Y	Z	Z	X	X	X	X
Ni(II)L_2	Y	Z	Z	X	X	X	X
Co(II) L_1L_2	Y	Z	Z	X	X	X	X
Mn(II) L_1L_2	Y	Z	Z	X	X	X	X
Ni(II) L_1L_2	Y	Z	Z	X	X	X	X

Key: X = Soluble, Z = slightly soluble, and Y = Insoluble

3.2 Infrared Spectra Results

Significant and useful information about the coordination reaction was provided by the IR spectra. Vibrational bands were present in all recorded spectra, primarily because of the N-H, O-H, C=O, C=N and N-N- groups as presented in **Figure 1 a-k** and summarized in **Table 3** (Aiyelabola *et al*., 2020; Sykula *et al*., 2023; Hosney *et al*., 2024). IR group vibrational bands of the free ligands: **L_1** and **L_2** were recorded and compared with both the single and mixed complexes of Co(II), Mn(II), and Ni(II). Due to intramolecular hydrogen bonding, **L_1** showed a broad vibrational band in the region of 3460 cm^{-1}. In contrast, **L_2** showed a somewhat narrow vibrational band because of the presence of fluoro on **L_2**, which can interfere with the hydrogen bond. The spectra of metal complexes showed persistence of this vibrational band, indicating that deprotonation had not taken place and that the hydroxyl group (-OH) was how the ligand and metal ion were coupled. The solid-state nature of the reaction media may have contributed to the non-deprotonation (Kitanosono and Kobayashi, 2021). However, in both single and mixed metal complexes, these vibration modes underwent a shift and emerged at a lower band, indicating the occurrence of complexation, which is consistent with the outcome of Santiago *et al*. (2020). Another vibrational band appeared in **L_1** and **L_2** at 1641 cm^{-1} and 1602 cm^{-1}, respectively, and is ascribed to √(C=N). These vibrational bands, however, changed and occurred at a lower frequency in single and mixed complexes. This suggests that azomethine nitrogen is involved in complexation, which is consistent with the findings of Uddin *et al*. (2019). In **L_1**, the vibrations caused by √(N-N) emerged at 778 cm^{-1}. Nevertheless, this vibration was not detected in **L_2**, suggesting that √(N-N) was not present in **L_2**. It was observed at higher frequencies in single metal complexes of **L_1** and mixed complexes, but at lower frequencies in single metal complexes of **L_2 due to** the presence of the fluoro group. The shift in the vibrational band suggests that N-N was involved in the complexation, which was consistent with the findings of Alzharani (2023). For Co(II), Mn(II), and Ni(II), the metal-oxygen bond appears at 513 cm^{-1}, 508 cm^{-1}, and 573 cm^{-1}, respectively, supporting the formation of M-O. For Co(II), Mn(II), and Ni(II), the metal-nitrogen band appears at 407 cm^{-1}, 427 cm^{-1}. The aforementioned bases proposed that the ligand chelates via C=N, the non-deprotonated hydroxyl group to the metal ion as bidentate ligands.

Table 3: Characteristic IR Spectra Bands (cm^{-1}) of Synthesised Ligands (**L_1** and **L_2**) and their Complexes

Compounds	**√(O-H)**	**√(C=N)**	**√(N-N)**	**√(C-C)**	**√(M-O)**	**√(M-N)**
L_1	3460	1641	778	1032		
L_2	3390	1602		1040		
Co(II)L_1	3412	1587	811	1027	508	417
Mn(II)L_1	3434	1583	812	1015	513	407
Ni(II)L_1	3414	1585	814	1017	517	403
Co(II)L_2	3410	1578	742	1019	525	460
Mn(II)L_2	3458	1584	751	1025	593	465
Ni(II)L_2	3494	1591	811	1027	573	517
Co(II) L_1L_2	3435	1583	812	1015	513	407
Mn(II) L_1L_2	3448	1600	782	1043	508	427
Ni(II) L_1L_2	3302	1591	811	1027	573	514

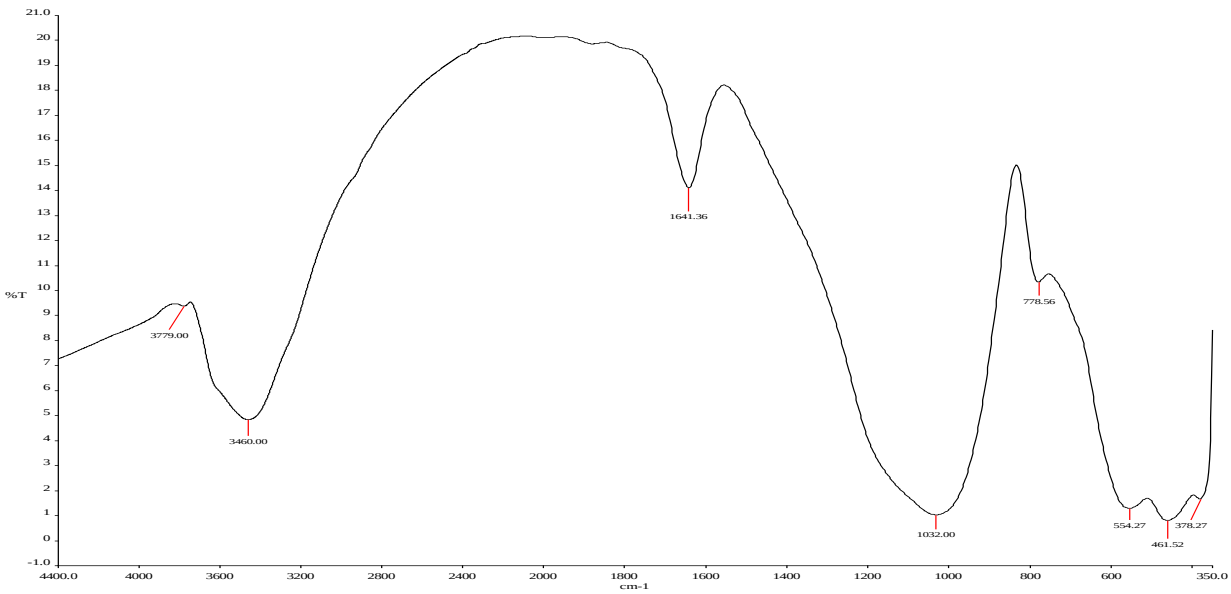

(a) IR Spectra of Ligand (**L_1**)

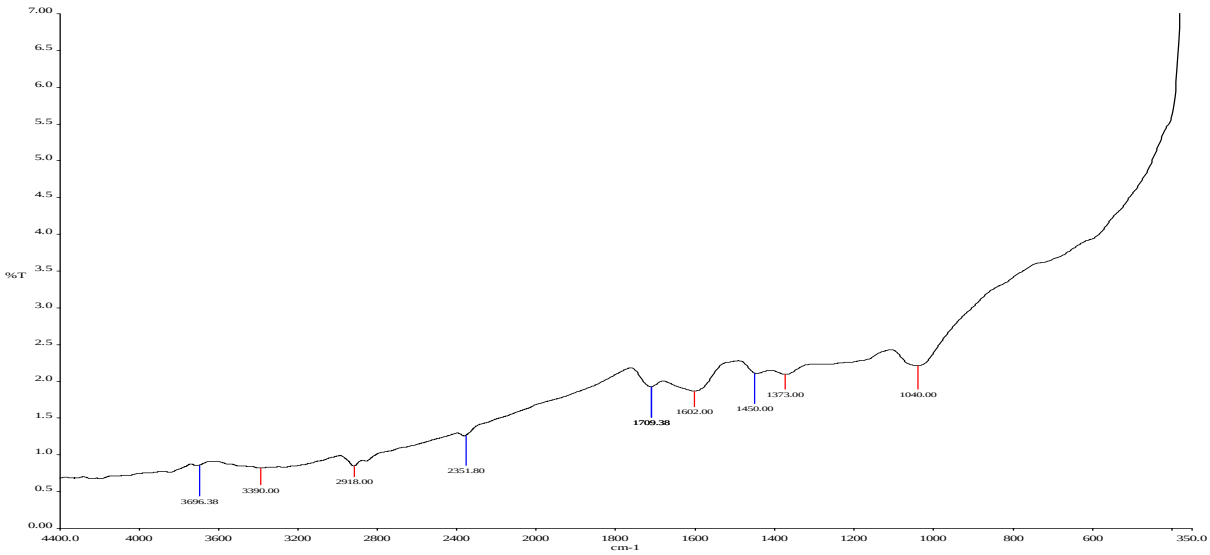

(b) IR Spectra of Ligand (**L**$_2$)

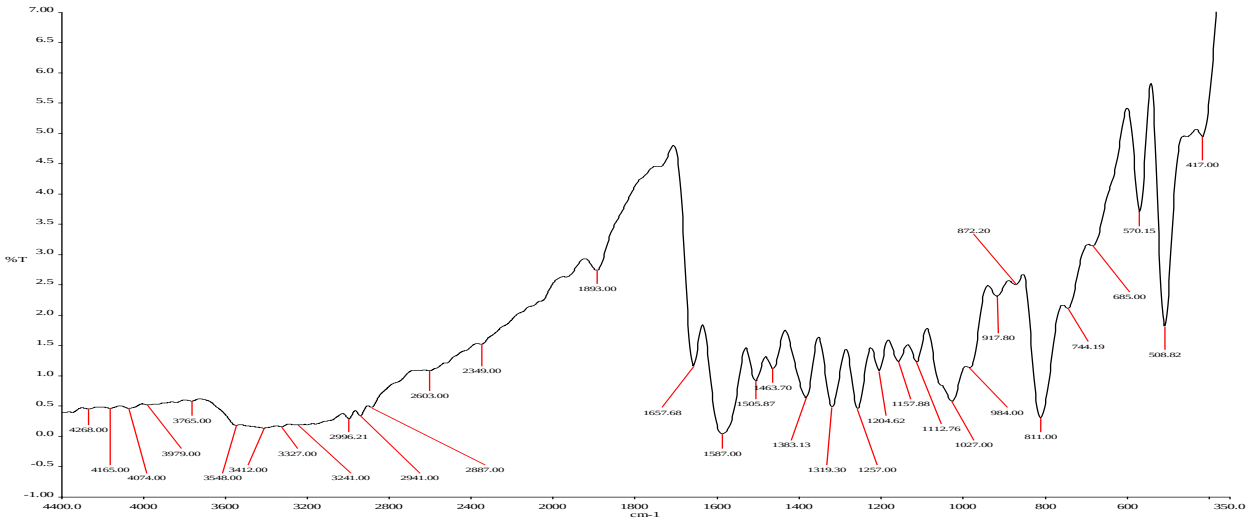

(c) IR Spectra of Co(II)L$_1$

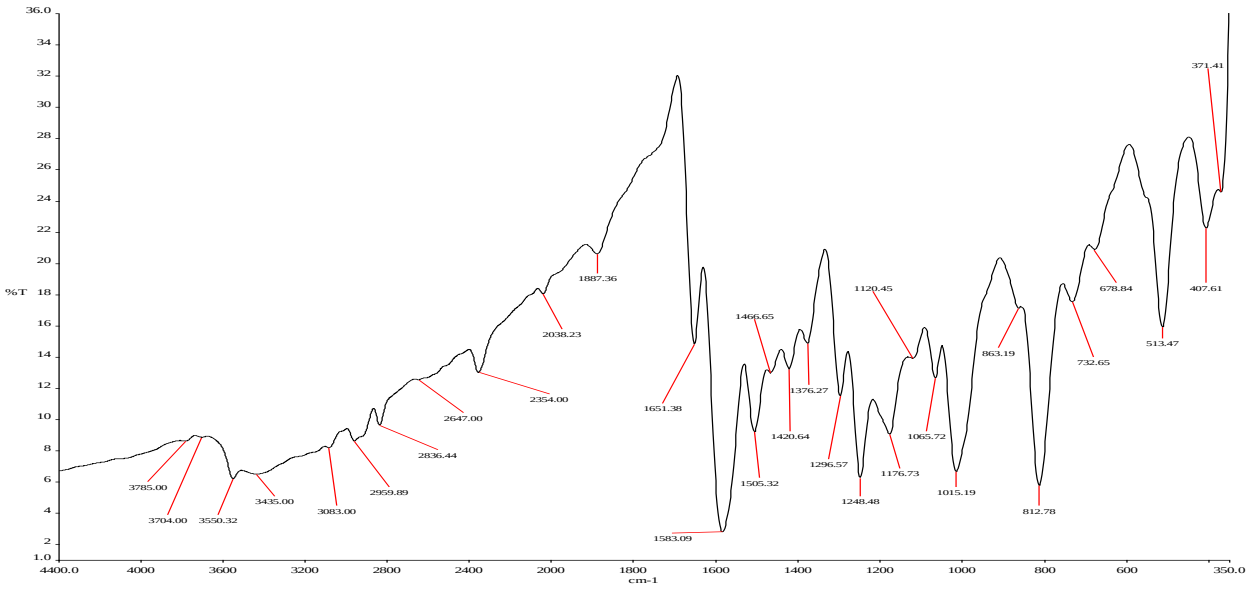

(d) IR Spectra of Mn(II)L$_1$

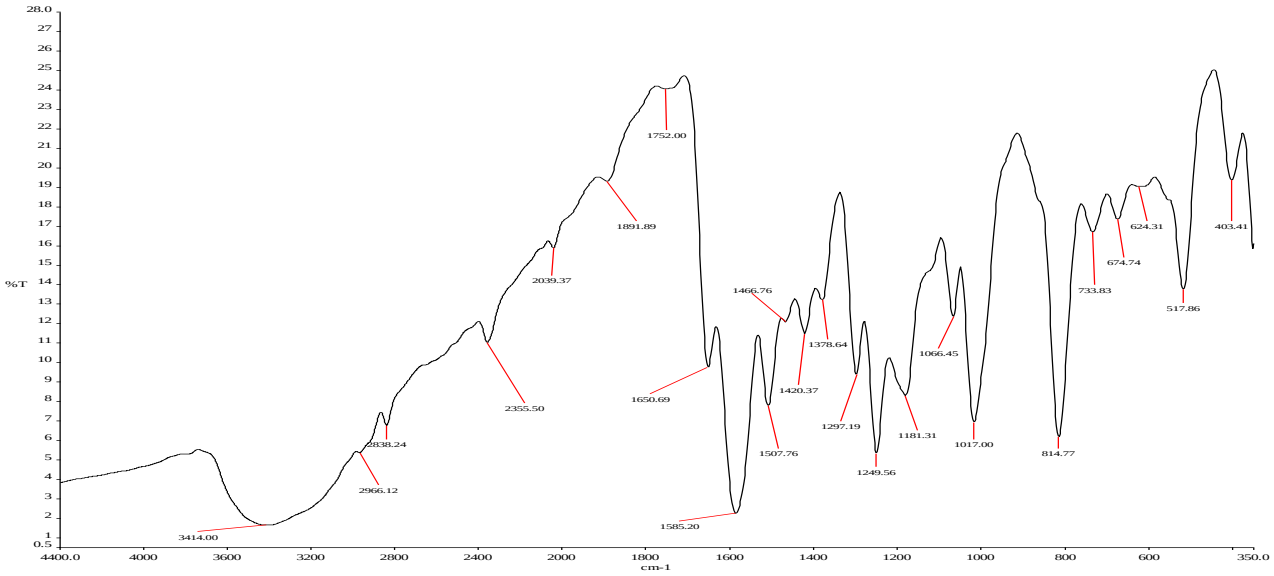

(e) IR Spectra of Ni(II)L_1

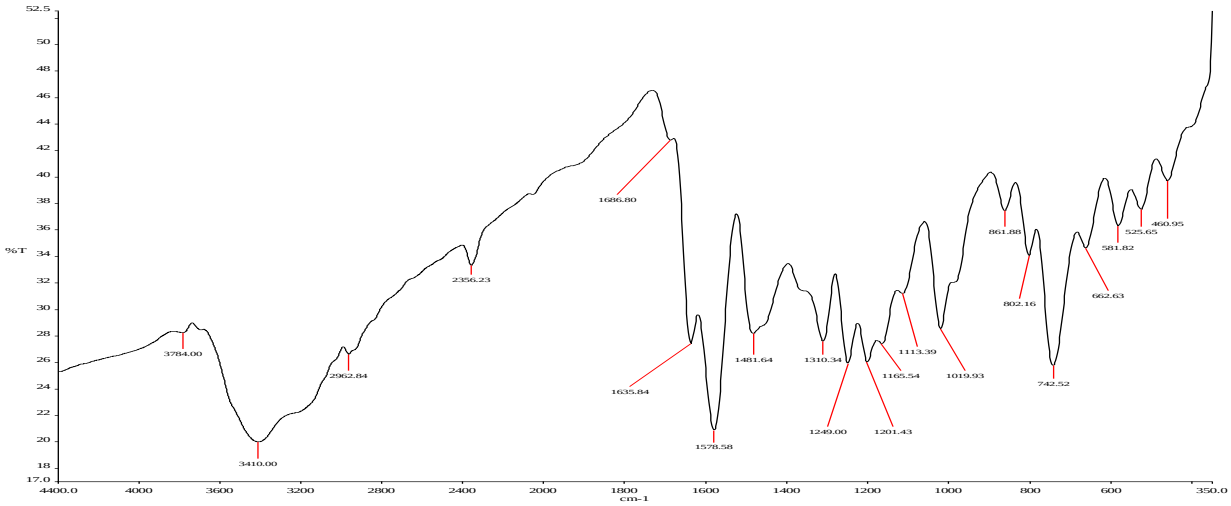

(f) IR Spectra of Co(II)L_2

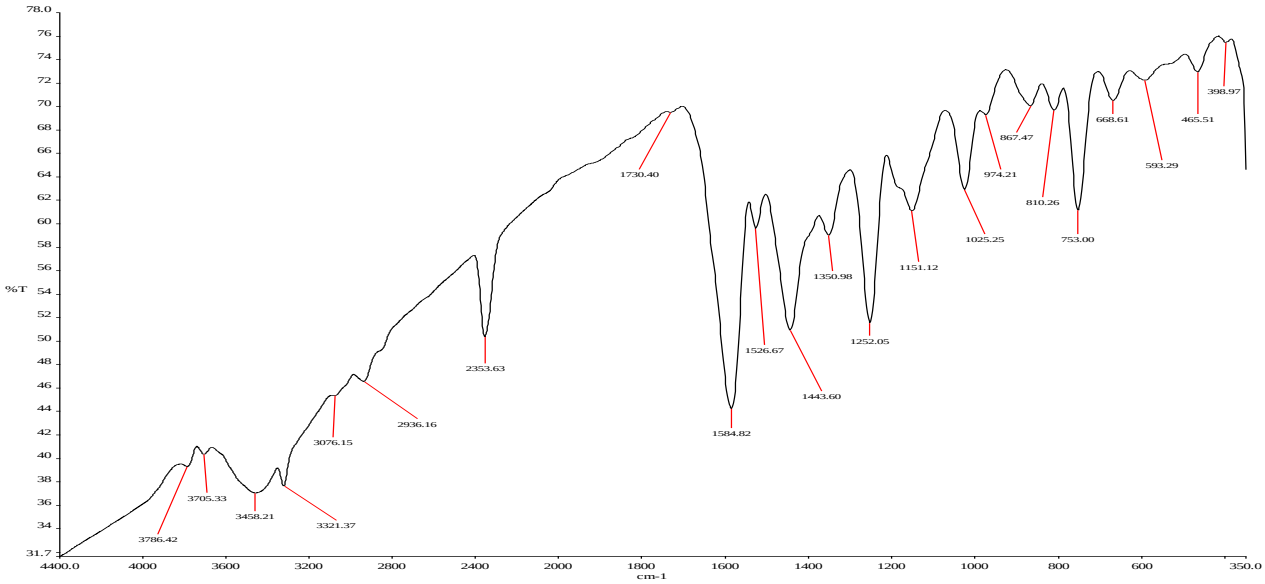

(g) IR Spectra of Mn(II)L_2

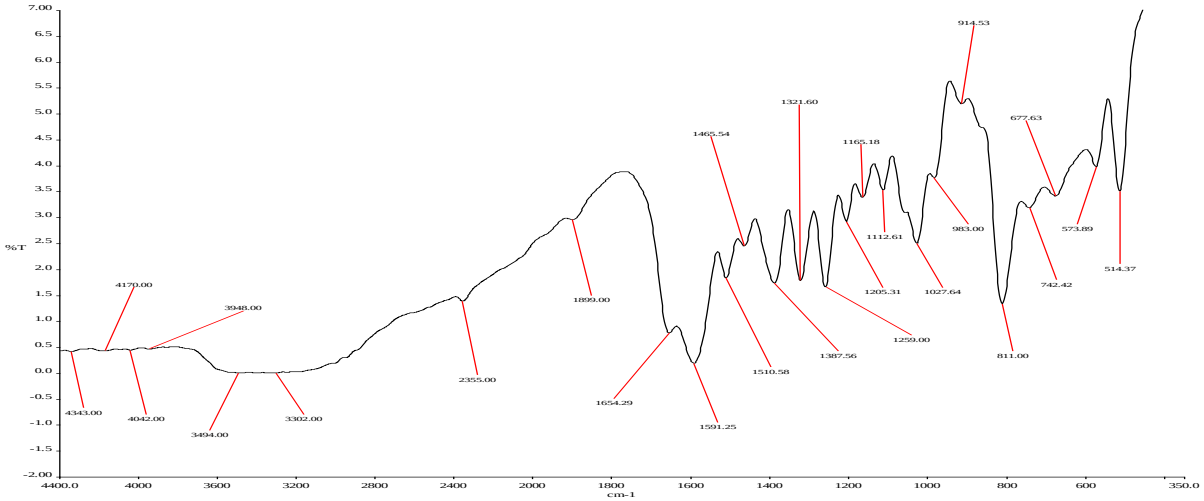

(h) IR Spectra of $Ni(II)L_2$

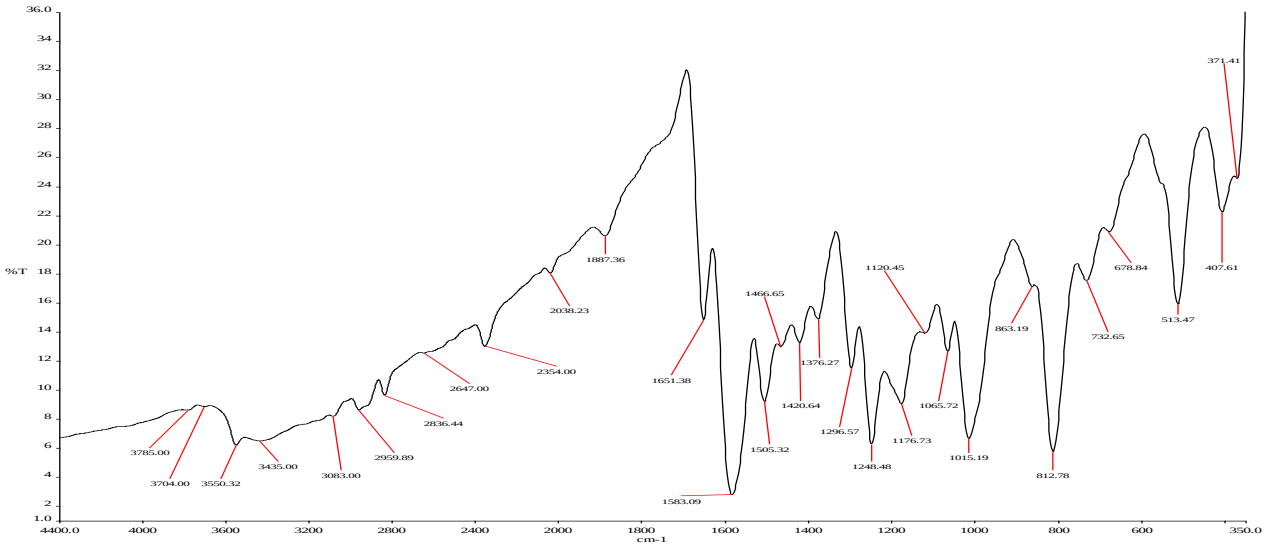

(i) IR Spectra of $Co(II)L_1L_2$ Complex

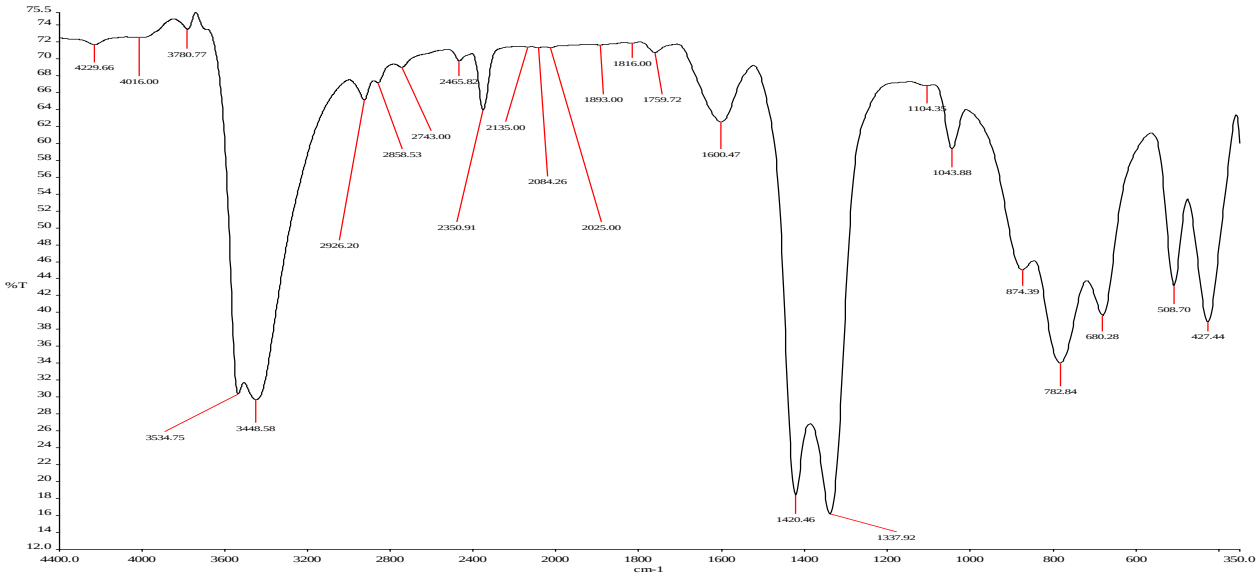

(j) IR Spectra of Mn(II) L_1L_2 Complex

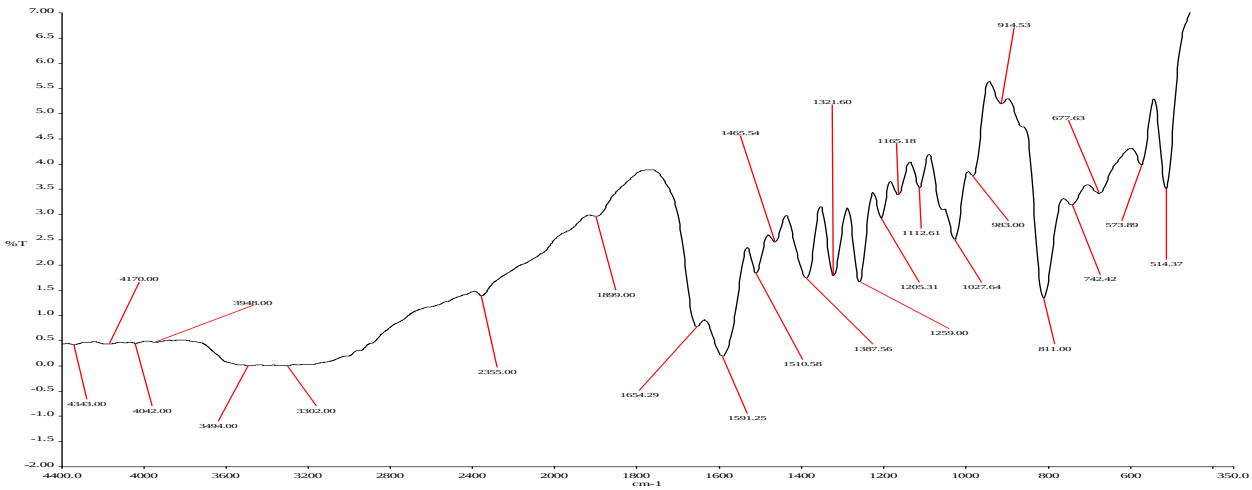

(k) IR Spectra of Ni(II) L_1L_2 Complex

Figure 1: IR Spectra (**a-k**) of L_1 and L_2 alongside their individual and mixed complexes with Co(II), Mn(II), and Ni(II)

3.3 The Electronic Spectra Results

Table 4 and **Figure 2 a-k** shows the electronic absorbance spectra for the free ligands **L_1** and **L_2**, along with the Co(II), Mn(II), and Ni(II) complexes, including the maximum band values for the ligands and complexes that were made. The UV/Vis spectra of the synthesised ligands: **L_1** and **L_2** revealed three bands at 209 nm, 214 nm, 218 nm and 205 nm, 213 nm, 345 nm which may be allotted to $n \rightarrow \pi^*$ of hydroxyl (-OH) and $\pi \rightarrow \pi^*$ transitions of phenyl (C=C), azomethane (HC=N) of **L_1** and **L_2** (Uddin *et al*., 2019; Bashir *et al*., 2023). Both the single and mixed metal complexes exhibit new absorption bands when compared to the ligands' adsorption bands. This is because the metal ions have complexed with **L_1** and **L_2**, shifting their absorption maxima to higher wavelengths Co(II) ions, which indicates bathochromic shift and complexation (El-Sonbati *et al*., 2022; Feryal and Alyaa, 2024). In contrast, Mn(II) and Ni(II) complexes also showed a new absorption band, indicating coordination with Mn(II) and Ni(II) ions. However, the absorption maxima of **L_1** and **L_2** shifted to a shorter wavelength, indicating a blue shift that could have been caused by complexation and the solvent effect (Bouchoucha *et al*., 2014; Kotynia *et al*., 2021).

Table 4: Electronic Spectral Data of Ligands (L_1 and L_2) and their Metal Complexes

Compounds	λ_{max}(nm)	Spectral Band(cm^{-1})	Assignment
L_1	209.50	47,733	$n \rightarrow \pi^*$
	214.00	46,729	$\pi \rightarrow \pi^*$
	218.50	45,767	$\pi \rightarrow \pi^*$
L_2	205.00	48,781	$n \rightarrow \pi^*$
	213.00	46,948	$\pi \rightarrow \pi^*$
	345.00	28,986	$\pi \rightarrow \pi^*$
Co(II)L_1	295.00	33,898	$n \rightarrow \pi^*$
	341.00	29,326	$\pi \rightarrow \pi^*$
	345.00	28,986	$\pi \rightarrow \pi^*$
Mn(II)L_1	199.00	50,251	$n \rightarrow \delta^*$
	243.00	41152	$n \rightarrow \pi^*$
	298.00	33,557	$\pi \rightarrow \pi^*$
	308.00	32,468	$\pi \rightarrow \pi^*$
Ni(II)L_1	191.00	52,356	$n \rightarrow \delta^*$

	200.00	50,000	$n \rightarrow \pi^*$
	218.00	45,872	$\pi \rightarrow \pi^*$
	228.00	43,860	$\pi \rightarrow \pi^*$
Co(II)L_2	201.00	49,751	$n \rightarrow \pi^*$
	215.00	46,512	$\pi \rightarrow \pi^*$
	271.00	36,900	$\pi \rightarrow \pi^*$
Mn(II)L_2	305.00	32,787	$n \rightarrow \pi^*$
	365.00	27,397	$\pi \rightarrow \pi^*$
	375.00	26,667	$\pi \rightarrow \pi^*$
N(II)L_2	239.00	41,841	$n \rightarrow \pi^*$
	285.00	35,088	$\pi \rightarrow \pi^*$
	299.00	33,445	$\pi \rightarrow \pi^*$
	331.00	30,212	$\pi \rightarrow \pi^*$
Co(II) L_1L_2	239.00	41,841	$n \rightarrow \pi^*$
	262.00	38,168	$n \rightarrow \pi^*$
	305.00	32,787	$\pi \rightarrow \pi^*$
	331.00	30,212	$\pi \rightarrow \pi^*$
Mn(II) L_1L_2	194.00	51,546	$n \rightarrow \delta^*$
	201.00	49,751	$n \rightarrow \pi^*$
	206.00	48,544	$\pi \rightarrow \pi^*$
	264.00	37,879	$\pi \rightarrow \pi^*$
Ni(II) L_1L_2	195.06	51,266	$n \rightarrow \delta^*$
	205.86	48,577	$n \rightarrow \pi^*$
	213.57	46,823	$\pi \rightarrow \pi^*$
	265.00	37,736	$\pi \rightarrow \pi^*$

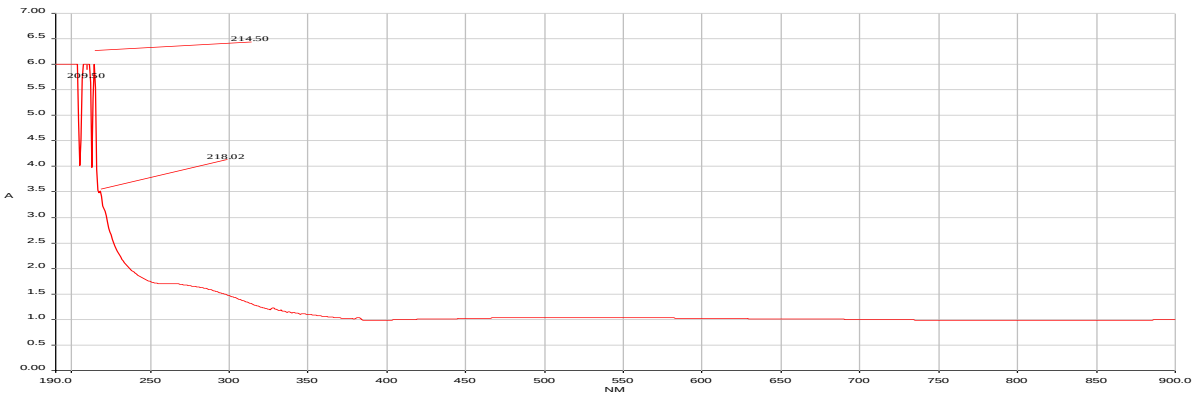

(a) UV Spectra of Ligand 1 (**L₁**)

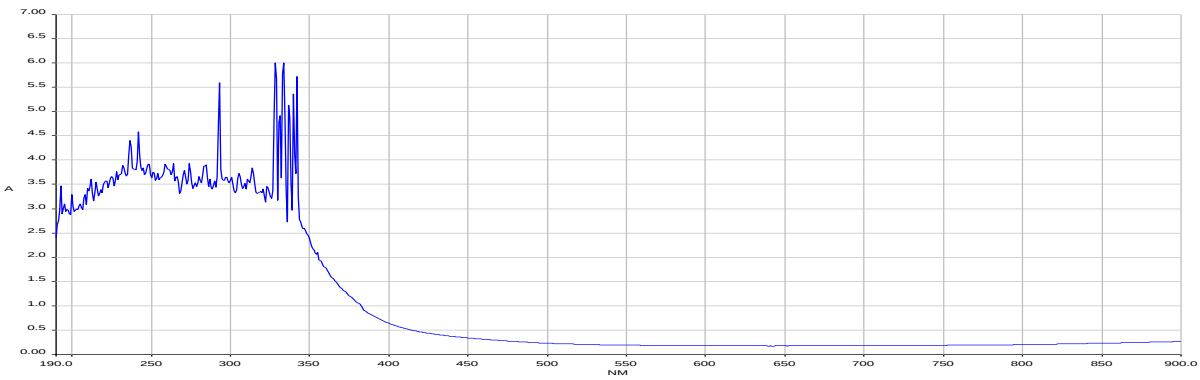

(b) UV Spectra of Ligand 2 (**L₂**)

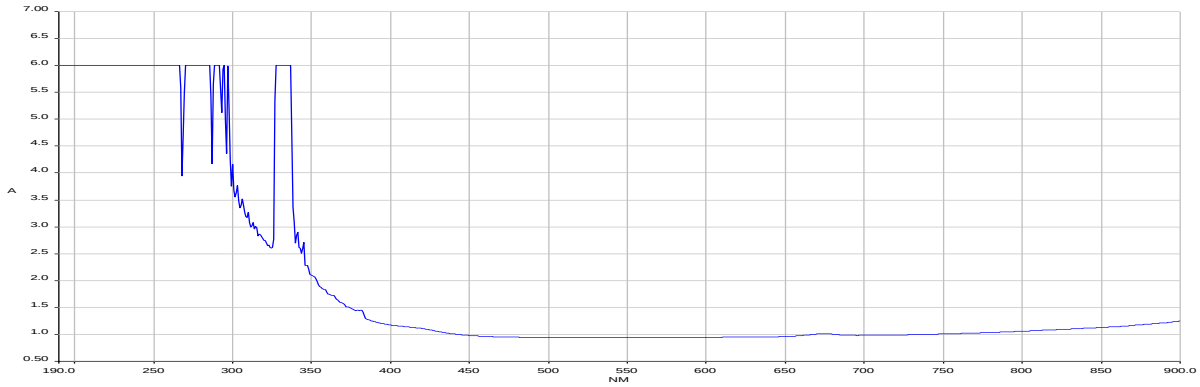

(c) UV Spectra of Co(II)L_1 Complex

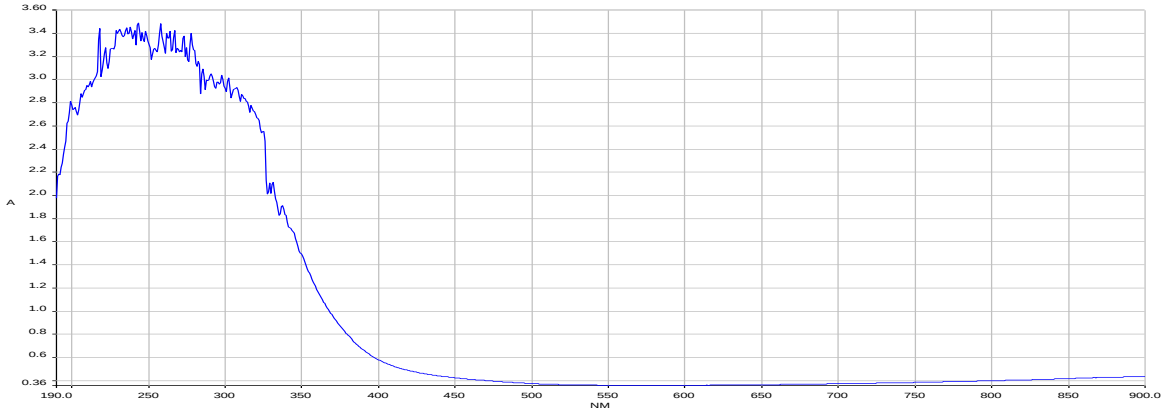

(d) UV Spectra of Mn(II)L_1 Complex

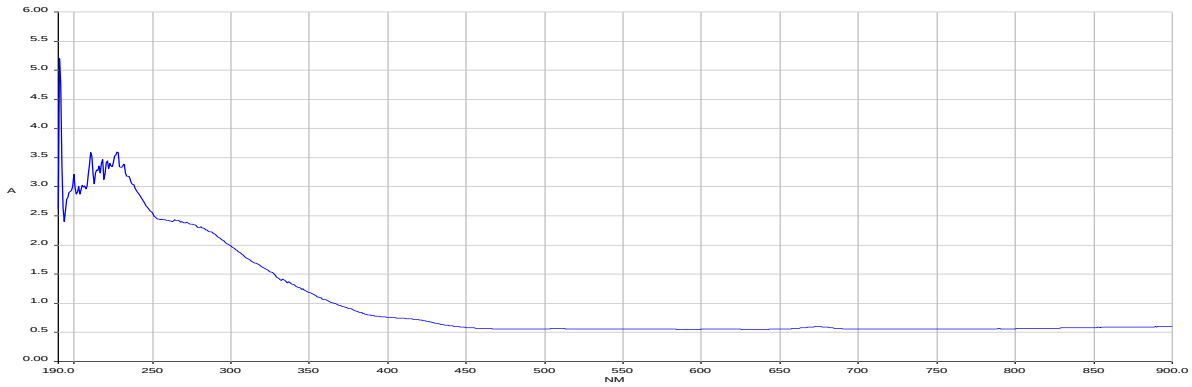

(e) UV Spectra of Ni(II)L_1 Complex

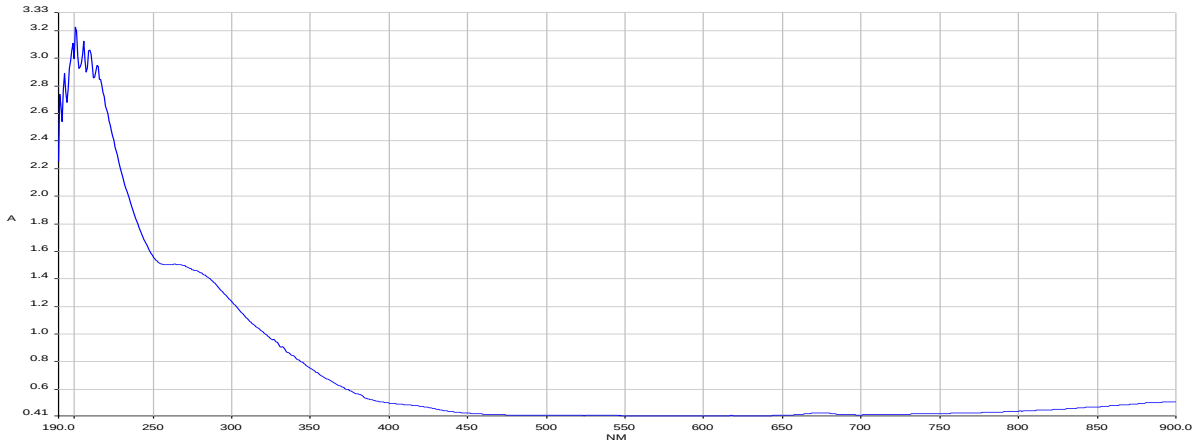

(f) UV Spectra of Co(II)L_2 Complex

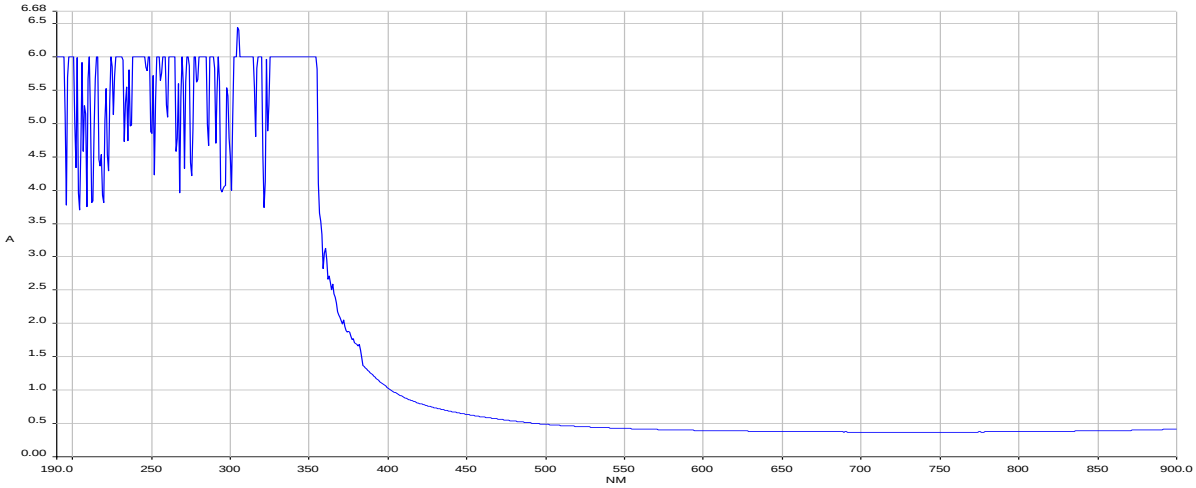

(g) UV Spectra of Mn(II)L_2 Complex

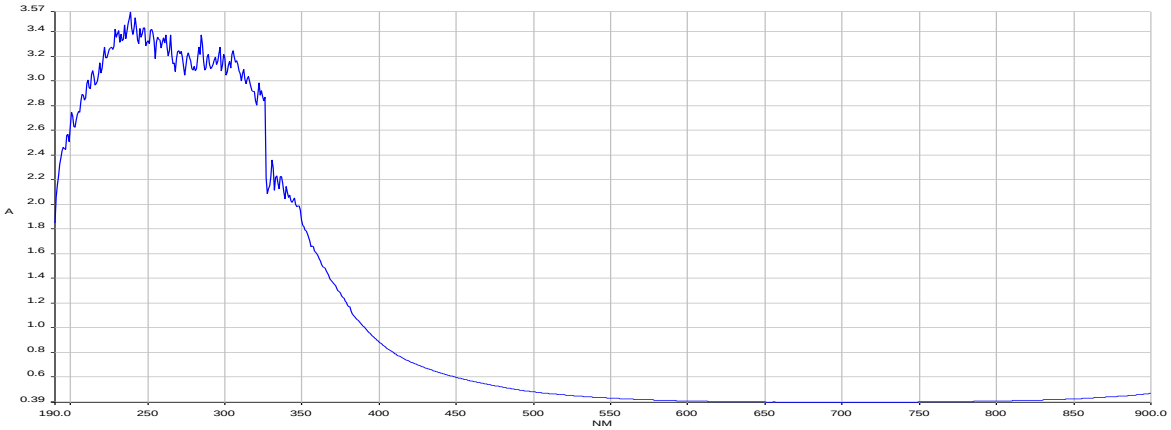

(h) UV Spectra of Ni(II)L_2 Complex

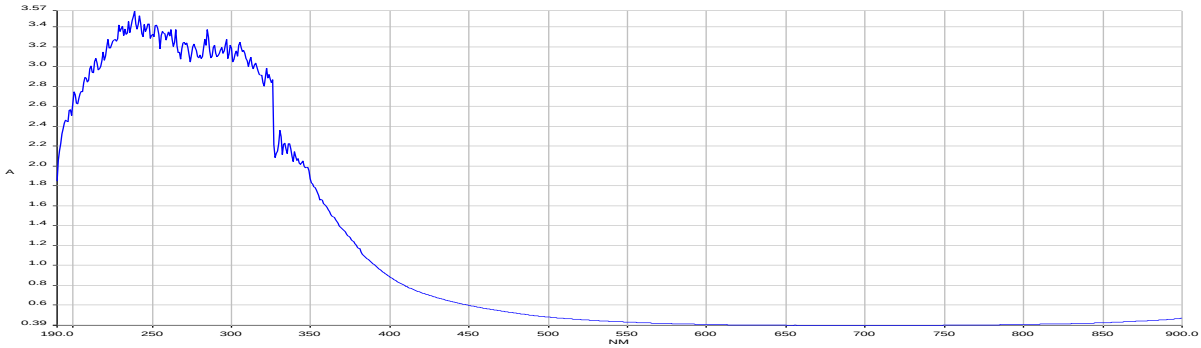

(i) UV Spectra of Co(II)L_1L_2 Complex

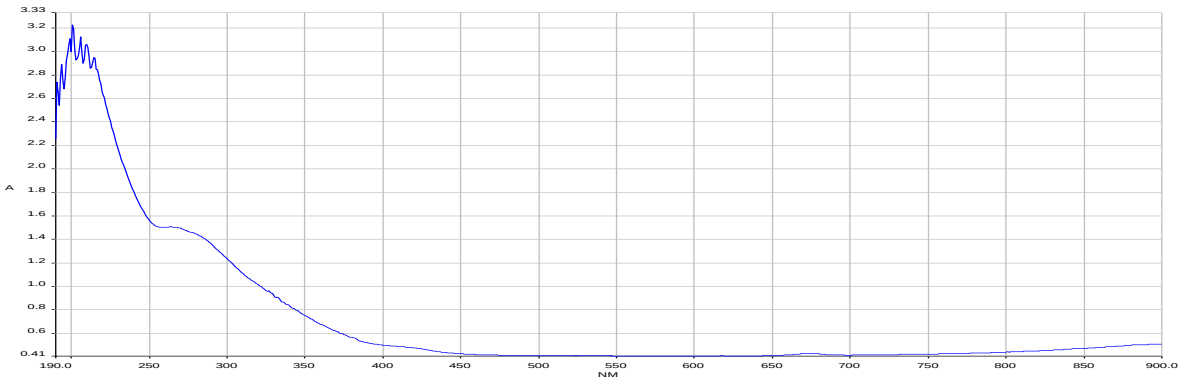

(j) UV Spectra of Mn(II) L_1L_2 Complex

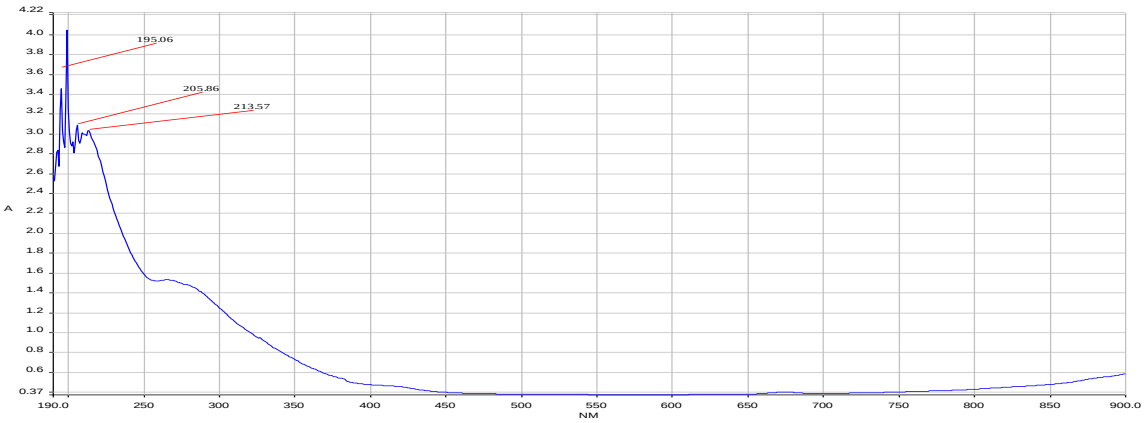

(k) UV Spectra of Ni(II) L_1L_2 Complex

Figure 2: UV Spectra (**a-k**) of L_1 and L_2 alongside their individual and mixed complexes with Co(II), Mn(II), and Ni(II)

3.4 Surface Morphology

Surface morphology of the synthesised ligands and complexes becomes more valuable and necessary due to the continuous shrinking of the material's dimension for copious applications going into the nanotechnology domain (Aldwayyan *et al.*, 2013; Khan *et al*., 2022; Saleh & Hassan, 2023). This study recorded SEM images to conduct morphological analyses of the synthesised ligands and complexes, aiming to ascertain whether complexation occurred during the grinding process. The micrograph (Figures 4a and b) shows the morphology of the ligands, while Figures 4c, d, and e expose the morphology of the metal complexes, which differ significantly from that of the ligand. This indicates the complexation of the ligands with the metal salts (formation of new products), which systematically fills the pores in the ligands (Figures 4a and b) (Mansour *et al*., 2024).

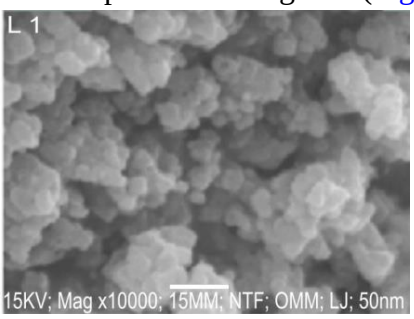

(a) Micrograph of L_1

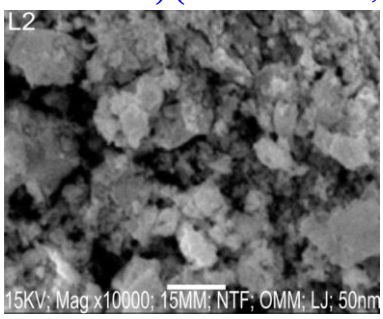

(b) Micrograph of L_2

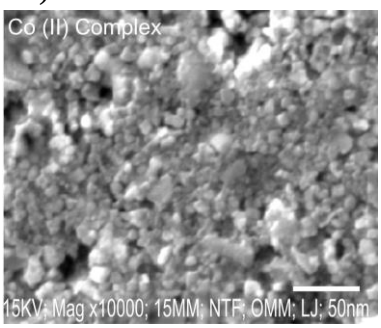

(c) Micrograph of Co (II) complex

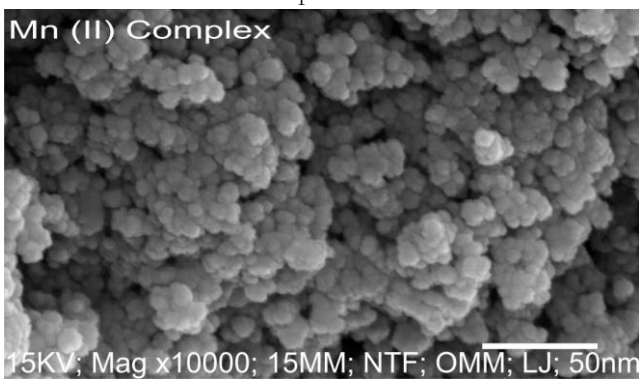

(d) Micrograph of Mn(II) complex

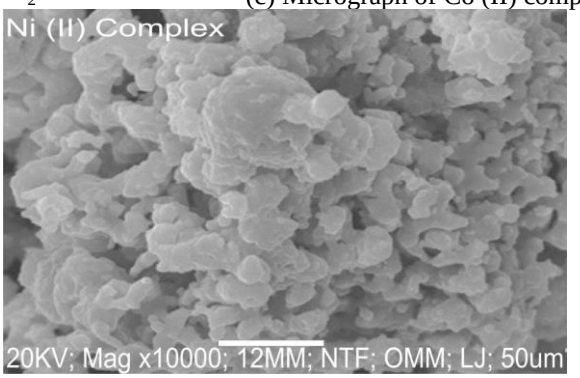

(e) Micrograph of Ni(II) complex

Figure 4: The SEM Images (Micrograph) of L_1 (4a), L_2 (4b), Co(II) (4c), Mn(II) (4d) and Ni(II) Complexes (4e)

The enhanced physical linkage of the ligands and metal salts during complexation is evident in the sectional pictures (Figures 4c, b, and e), causing a decrease in pore diameters and particle interaction. The cross-sectional image of the ligands shows many holes of different sizes, which are larger than the pores seen in the imaginings of the metal complexes. Since metal salts are occupying the ligand's pores, this indicates a reduction in porosity due to complexation. The structural ligands resembled a cluster of needles emanating from a certain location. It was notably practical that each needle varies in both diameter and length (Iorungwa *et al*., 2024). The clear differences in the shape of ligands and metal complexes show that complexes are being formed. The SEM micrographs illustrated the changes in texture and morphology resulting from the combination of ligands and metal salts during the grinding synthesis of the complexes, as seen in Figures 4c, d, and e. The findings indicate that the morphology and dimensions of the particles altered during the complexation process (Chaudhary and Mishra, 2017). The micrograph of L_1 (Figure 4a and b) illustrates the many forms of crystals.

3.5 Ovicidal and Larvicidal Activities

Owing to the limited environs available for mosquito ova and larvae, studies have suggested that mosquito control should begin at these early developmental stages (Antonio-Nkondjio *et al*., 2018; Wang *et al*., 2020; Dusfour and Chaney, 2022). Since mosquito eggs develop resistance upon solidification, ovicidal activity was carried out on freshly laid eggs (Ramkumar *et al*., 2019; Yang *et al*., 2021). This study investigated the ovicidal properties of hydrazone ligand and its single and mixed metal complexes against the eggs of *Anopheles gambiae* and *Culex quinquefasciatus*, with 25 eggs of each species individually exposed to four concentrations (62.5, 125, 250, and 500 mg/L) and each concentration replicated five times to determine hatchability rates. After 24 h of exposure, ovicidal activity increased significantly with increasing concentrations, with *C. quinquefasciatus* eggs showing a minimum of 25 % ovicidal activity at 62.5 mg/L of ligand 2 (L_2) and a maximum of 100 % at 500 mg/L of the $Co(II)L_1L_2$ complex, indicating the enhanced efficacy of mixed complexes over single complexes. As shown in Figure 6, the order of ovicidal activity for *C. quinquefasciatus* eggs was $Co(II)L_1L_2$ (100 %) > $Ni(II)L_1L_2$ (84 %) > $Mn(II)L_1L_2$, $Co(II)L_2$ (82 %) > $Mn(II)L_1$ (81 %) > $Mn(II)L_2$ (80 %) > $Co(II)L_1$, $Ni(II)L_2$, L_2, L_1 (78 %) > $Ni(II)L_1$ (75%). However, despite the general trend of increased activity upon complexation, *A. gambiae* exhibited lower ovicidal susceptibility than *C. quinquefasciatus*, with the lowest ovicidal activity (25 %) observed at 62.5 mg/L of $Ni(II)L_1L_2$ and the highest activity (83 %) recorded at 500 mg/L of L_1, this is due to the chemical composition of *A. gambiae* eggs showing stronger affinity for the functional groups in L_1, as represented in **Figure 7** (Ahouandjinou *et al*., 2024; Takken *et al*., 2024). The ovicidal efficacy followed the order: L_1 (83 %) > $Ni(II)L_1L_2$ (81 %) > $Mn(II)L_1L_2$ (80 %) > $Co(II)L_1L_2$ (79 %) > $Ni(II)L_2$ (76 %) > $Co(II)L_1$, $Mn(II)L_1$, $Ni(II)L_1$, $Co(II)L_2$ (75 %) > $Co(II)L_2$, L_2 (73 %), further confirming that mixed complexes were more effective than single complexes against *A. gambiae* eggs at 500 mg/L. Furthermore, the positive control, azadirachtin, exhibited 100% ovicidal efficacy at a much lower concentration of 10 mg/L against both *C. quinquefasciatus* and *A. gambiae* eggs, marking the potential of hydrazone-based metal complexes as promising ovicidal agents, with mixed complexes demonstrating superior efficacy over their single-complex equivalent. This study examined the larvicidal action of ligands and their complexes against the larvae of two kinds of mosquitoes. *Anopheles gambiae* and *Culex quinquefasciatus* larvae totalling twenty-five were individually treated to four concentrations: 62.5, 125, 250, and 500 mg/L. The mosquito larvae's mortality was measured in percentages after each concentration was repeated five times. After exposing the larvicidal activities to hydrazone ligands and their complexes for 24 h, there

was a notable rise in the mortality percentage with concentration. This is consistent with the findings of Ravindran *et al* (2020).

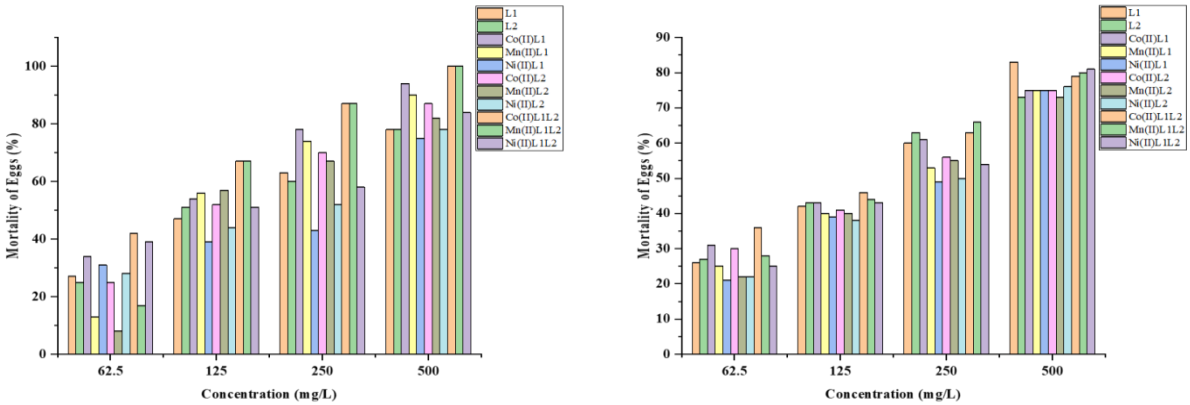

(a) The Ovicidal Activity of the two Ligands and their Complexes against *C. quinquefaciatus* Eggs at different Concentrations.

(b) The Ovicidal Activity of the two Ligands and their Complexes against *A. gambiae* Eggs at different Concentrations.

Figure 6: The Ovicidal Activity (%) of the two Ligands, and their Complexes against the Larvae of *C. quinquefasciatus* (6a) and *A. gambiae* (6b) at different Concentrations.

When the tested hydrazone ligands and their complexes were compared, the maximum larvicidal activity (82 %) was observed against *C. quinquefasciatus* at 500.00 mg/L of Co(II)L_1L_2, indicating enhanced activity on complexation of the mixed complexes than the single complexes. As shown in Figure 7a, the order of enhanced activity on complexation was Co(II)L_1L_2 (82 %) > Ni(II) L_1L_2 (79 %) > Mn(II) L_1L_2 (68 %) > Co(II)L_1(67 %) > Ni(II) L_1, Co(II)L_2 (66 %) > Mn(II)L_2, Ni(II)L_2 (65 %) >L_2 (64 %)> Mn(II)L_1 (62 %) > L_1 (61 %). *A. gambiae* was found to have lower larvicidal activity (3 %) than *C. quinquefasciatus*, as shown in Figure 7b. The lowest larvicidal activity (3 %) was recorded at 62.50 mg/L of ligand 1 (L_1). With 500.00 mg/L of Mn(II) L_1L_2 (54 %) having the highest larvicidal activity against *A. gambiae*, there was increased activity with complexation, with Mn(II) L_1L_2 (54 %) > Ni(II)L_1L_2 (53 %) > Co(II)L_1L_2 (50 %) > Mn(II)L_1, Mn(II)L_2 (49 %) > Ni(II)L_2 (47 %) > Ni(II)L_2 (46 %) > Co(II)L_2 (40 %) > L_2 (39%) > Co(II)L_2 (35 %) > L_1 (30%). This implies that different species of mosquitoes may be more or less sensitive to hydrazone ligands and their complexes (Amer and Mehlhorn, 2006). It was discovered that *A. gambiae larvae* were the least susceptible to the hydrazone ligands and their complexes, followed by *Culex quinquefasciatus*.

The obtained results were consistent with those of Derua *et al*. (2021), who discovered that Culex *quinquefasciatus* was much more susceptible to *Bacillus thuringiensis Vari Israelensis* than *A. gambiae* at both lethal dosages (L_{50} and L_{95}). Conversely, Sillo *et al*. (2019) observed that the root extract of Hypoestes forskaolii chloroform exhibited notably greater larvicidal action against A. gambiae than C. quinquefasciatus after 72 h of exposure. Additionally, Snaha *et al*. (2022) found that essential oils exhibited a larvicidal impact with LC_{50} values that were more sensitive to *Culex* and *Aedis*, even if *Armigeres* was more resistant. Furthermore, the extraction solvent may affect the toxicity against the vector because different organic solvents show different polarity gradients when dissolving hazardous components (Venkatesan *et al*., 2019; Aboagye *et al*., 2021). Therefore, careful thought must be given to the solvent utilised in synthesizing hydrazone ligands and their complexes before determining any potential larvicidal effects.

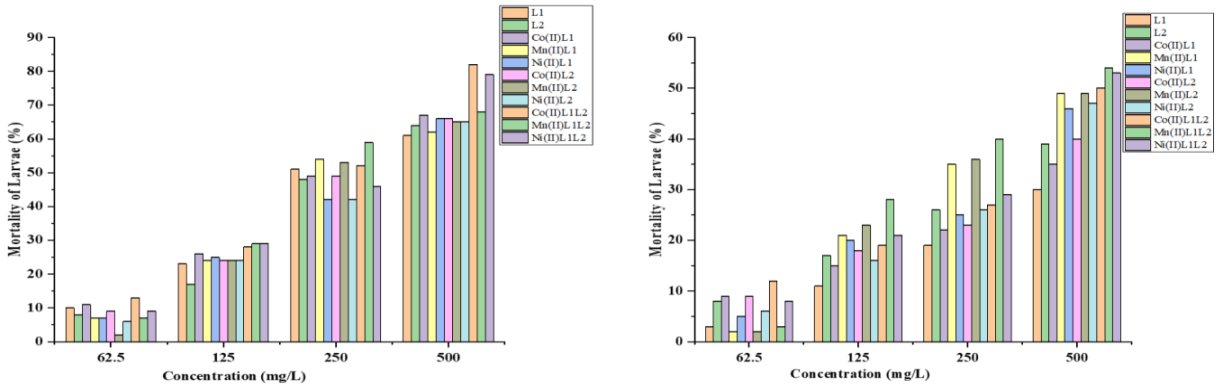

(a) The Larvicidal Activity of the two Ligands and their Complexes against *C. quinquefaciatus* Larvae at different Concentrations.

(b) The Larvicidal Activity of the two Ligands and their Complexes against *A. gambiae* Larvae at different Concentrations.

Figure 7: The Larvicidal Activity (%) of the two Ligands, and their Complexes against the Larvae of *C. quinquefasciatus* (7a) and *A. gambiae* (7b) at different Concentrations.

Conclusion

Two ligands, L_1 and L_2, and their single and mixed complexes of Co(II), Mn(II), and Ni(II) were synthesized without the use of solvents. The ligands and their complexes underwent characterization and testing for their antimalarial activities (ovicidal and larvicidal). The colours of the starting materials and products demonstrated that reactions took place during the grinding synthesis. The solubility result of ligands and their complexes showed their nonpolarity, which was supported by the molar conductivity data, which indicated that they were non-electrolytic. The infrared (IR) finding showed that the hydroxyl group and the azomethine nitrogen were the pathways through which the Co(II), Mn(II), and Ni(II) ions were chelated, demonstrating the bidentate character of the two ligands. The chelation of the two ligands and metal ions was confirmed by a shift from lower to higher frequencies in the electronic spectra of the free ligands when compared to complexes utilizing different transitions. The result of the ovicidal activity was higher against *C. quinquefasciatus* eggs compared *to A. gambiae*. The synthesized ligands and their single and mixed complexes were found to be more effective against *C. quinquefasciatus* than *A. gambiae*, demonstrating that the mosquito species affected the ligands' effectiveness and their complexes. The synthesised ligands and complexes are potential control agents for an integrated mosquito management program, as evidenced by their activities and direct proportionality to concentration increase in larvicide and ovicide efficacy.

Conflict of interest

The authors declare that they have no conflict of interest

References

Aboagye, E. A., Chea, J. D. and Yenkie, K. M. (2021) Systems level roadmap for solvent recovery and reuse in industries, *Science*, 24 (10), 103114, https://doi.org/10.1016/j.isci.2021.103114

Ahouandjinou, M.J., Sovi, A., Sidick, A., Sewadé, W., Koukpo, C. Z., Chitou, S., Towakinou, L., Adjottin, B., Steve Hougbe, S., Filémon Tokponnon, F., Padonou, G. G., Akogbéto, M., Messenger, L. A., and Ossè, R. A. (2024) First report of natural infection of *Anopheles gambiae s.s.* and *Anopheles coluzzii* by *Wolbachia* and Microsporidia in Benin: a cross-sectional study. *Malaria Journal*, 23, 72. https://doi.org/10.1186/s12936-024-04906-1

Aiyelabola, T. O., Akinkunmi, E. O. and Akinade, R. (2020). Syntheses of coordination compounds of (±)-2-amino-3-(4-hydroxyphenyl) propionic acid, mixed ligand complexes and their biological activities. *Advances in Biological Chemistry*, 10, 25-42.

Aldwayyan A.S., Al-Jekhedab F.M., Al-Noaimi M., *et al*. (2013), Synthesis and Characterization of CdO Nanoparticles Starting from Organometalic Dmphen-CdI2 complex, *Int. J. Electrochem. Sci.*, 8 N°8, 10506-10514. https://doi.org/10.1016/S1452-3981(23)13126-9

Alshahateet S.F., Altarawneh R.M., Al-Tawarh W.M., Al-Trawneh S.A., Al-Taweel S., Azzaoui K., Merzouki M., Sabbahi R., Hammouti B., Hanbali G., Jodeh S. (2024), Catalytic green synthesis of Tin(IV) Oxide nanoparticles for phenolic compounds removal and molecular docking with EGFR Tyrosine Kinase, *Scientific reports*, 14(1), 6519, https://doi.org/10.1038/s41598-024-55460-4

Alshahateet S.F., Al-Trawneh S.A., Er-rajy M., Zerrouk M., Azzaoui K., Al-Tawarh W.M., Hammouti B., Salghi R., Sabbahi R., Alanazi M.M., et al. (2024b) Green Synthesis of Zinc Oxide Nanoparticles for Tetracycline Adsorption: Experimental Insights and DFT Study. *Plants.* 13(23), 3386. https://doi.org/10.3390/plants13233386

Alzharani, A. A. (2023) Three Cu (II)-hydrazone complexes: synthesis, physicochemical characteristics, stability, thermal analysis, and investigation of metal and iodine absorption. *Journal of Umm Al-Qura University Appllied Science*. https://doi.org/10.1007/s43994-023-00054-5

Amer A. and Mehlhorn H., (2007) Larvicidal effect of various essential oils against *Aedes*, *Anopheles* and *Culex Larvae* (Diptera: Culicidae). *Parasitology Research*, 99, 466-472. http://dx.doi.org/10.1007/s00436-006-0182-3.

Anand, S., Chris, W. and Snyder, J. (2022) Thermodynamic guidelines for maximum solubility. *Chemistry of Materials*, 34 (4), 1638-1648.

Andriianova, A. N., Biglova, Y. N. and Mustaffin, A. G. (2020). Effect of structural factors on the physicochemical properties of functionalized polyanilines. *RSC Advances*, 10 (13), 7468-7491.

Antonio-Nkondjio, C., Sandjo, N. N., Awono-Ambene, P. and Wondji, C. S. (2018) Implementing a larviciding efficacy or effectiveness control intervention against malaria vectors: key parameters for success. *Parasite & Vectors*, 11 (57),

Araújo, M. S., Gil, L. H. and Silva, A. A. (2012) Larval food quantity affects development time, survival and adult biological traits that influence the vectorial capacity of *Anolpheles darling* under laboratory conditions. *Malaria Journal*, 11, 261-270.

Atabo, S., Manyi, M. and Egbodo, S. (2019) Evaluation of bioactive composition and larvicidal activities of *Garcinia kola* seeds on F2 *Anopheles gambiae* complex larvae (Diptera: Culicidae). *Journal of Biologically Active Products from Nature*, 9 (4), 289-298.

Barbara, M. (2020) Homo- and Hetero-Oligonuclear Complexes of Platinum Group Metals (PGM) Coordinated by Imine Schiff Base Ligands. *International journal of molecular science*, 21 (3493), 1-28

Bashir, M., Dar, A. A. and Yousuf, I. (2023) Syntheses, structural characterization, and cytotoxicity assessment of novel Mn(II) and Zn(II) complexes of aroyl-hydrazone Schiff Base ligand. *ACS Omega*, 8 (3), 3026-3042; doi: 10.1021/acsomega.2c05927.

Bouchoucha, A., Terbouche, A., Bourouina, A.and Djebbar, S. (2014) New complexes of manganese (II), nickel (II) and copper (II) with derived benzoxazole ligands: Synthesis, characterization, DFT, antimicrobial activity, acute and subacute toxicity. *Inorganica Chimica Acta*, 418, 187-197. https://doi.org/10.1016/j.ica.2014.04.016

Brum, J. O., Franca, T. C., Laplante, S. R. and Villar, J. D. (2020) Synthesis and biological activity of hydrazones and derivatives: A review. *Mini Review Medicinal Chemistry*, 20 (5), 342-368. DOI: 10.2174/1389557519666191014142448

Chaudhary N. K. and Mishra P., (2017). Metal complexes of novel Schiff based on penicillin: Characterization, molecular modeling, and antibacterial activity study. *Bioinorganic Chemistry and Applications*, 2017, 6927675

Chaouiki A., Chafiq M., Lgaz H., Al-Hadeethi M.R., Ali I.H., Masroor S., Chung I-M. (2020). Green Corrosion Inhibition of Mild Steel by Hydrazone Derivatives in 1.0 M HCl. *Coatings*, 10(7), 640. https://doi.org/10.3390/coatings10070640

Dafa, S. T., Iorungwa, M. S., Wuana, R. A., Iornumbe, E. N., Ahile, U. J. and Akoso, N. V. (2023) A review on mortar-pestle grinding synthesis and thermal profiling of hydrazone-based complexes as biocidal agents. *Nigerian Research Journal of Chemical Sciences*, 11 (2), 234-251.

Das, B., Baidya, A. T. K., Mathew, A. T., Yadav, A. K. and Kumar, R. (2022) Stuctural modification aimed for improving solubility of lead compounds in early phase drug discovery. *Journal of Bioorganic and Medicinal Chemistry*, 56, 116614.

Derua, Y. A., Kweka, E. J., Kisinza, W. N., Yan, G., Githoko, A. K. and Mosha, F. W. (2021) The effect of coexistence between larvae of *Anopheles gambiae* and *Culex quinquefasciatus* on larvicidal efficacy of Bacillus thuringiensis var. israelensis. *Journal of East Africa Science*, 3(1), **DOI** https://doi.org/10.24248/EASci-D-20-00011

Dusfour I. and Chaney S. C., (2022) Mosquito control: Success, failure and expectations in the context of arbovirus expansion and emergence. In: Hall M, Tamïr D, editors. Mosquitopia: The Place of Pests in a Healthy World [Internet]. New York: Routledge. Chapter 14. Available from: https://www.ncbi.nlm.nih.gov/books/NBK585173/ doi: 10.4324/9781003056034-19

El-Barasi, N. M., Miloud, M. M., El-ajaily, M. M., Mohapatra, R. K., Sarangi, A. K., Das, D., Mahal, A., Parhi, P. K., Pintilie, L., Barik, S. R., Amin Bitu, M. N., Kudrat-E-Zahan, M., Tabassum, Z., Al-Resayes, S. I. and Azam, M. (2020) Synthesis, structural investigations and antimicrobial studies of hydrazone-based ternary complexes with Cr(III), Fe(III) and La(III) ions. *Journal of Saudi Chemical Society*, 24(6), 492-503. https://doi.org/10.1016/j.jscs.2020.04.005

El-khlifi A., Zouhair F. Z., Al-Hadeethi M. R., Lgaz H., Lee H-S., Salghi R., Hammouti B., Erramli H. (2024) Assessment of Hydrazone Derivatives for Enhanced Steel Corrosion Resistance in 15 wt.% HCl Environments: A Dual Experimental and Theoretical, *Molecules*, 29, 985. https://doi.org/10.3390/molecules29050985,

El-Sonbati, A., El-Mogazy, M., Nozha, S., Diab, M., Abou-Dobara, M., Eldesoky, A.and Morgan, S. (2022) Mixed ligand transition metal(II) complexes: Characterization, spectral, electrochemical studies, molecular docking and bacteriological application. *Journal of Molecular Structure*, 1248, 131498. https://doi.org/10.1016/j.molstruc.2021.131498

Feryal A. M. and Alyaa S.M.O.A., (2024).Divalent transition metal complexes with mixed of β-enaminone and N,O-donor ligands: synthesis, characterization and biological assessment. *Bullettin Chemical Society Ethiopia*, 39(1), 65-78.

Heinz B. (2014). Counting ions' in Alfred Werner's coordination chemistry using electrical conductivity measurements. *Educación QuíMica*, 25, 267-275. https://doi.org/10.1016/S0187-893X(14)70567-1

Heuer-Jungermanm, A., Feliu, N., Bakaimi, I., Hamaly, M., Alkilany, A., Chakraborty, I., Masood, A., Casula, M. F., Kostopoulou, A., Oh, E., Susumu, K., Stewart, M. H., Medintz, I. L., Stratakis, E., Parak, W. J. and Kanaras, A. G. (2019) The role of ligands in the chemical synthesis and applications of inganic nanoparticles. *Chemical Review*, 119 (8), 4819-4880.

Hosny, N. M., Samir, G. and Abdel-Rhman, M. H. (2024) *N*-(Furan-2-ylmethylene)-2-hydroxybenzo hydrazide and its metal complexes: synthesis, spectroscopic investigations, DFT calculations and cytotoxicity profiling. *BMC Chemistry*, 18, 22-36.

Iorungwa, M. S., Abuh, H., Wuana, R. A., Amua, Q. M., Iorungwa, P. D. and Danat, B. T. (2024) Solvent- Free Synthesis, Characterization, Thermogravimetric and Antimicrobial Studies of Cu(II) Complex with Imine Ligands. *ChemSearch Journa*l 15(1), 135-143

Iorungwa, M. S., Wuana, A. R., Tyagher, L., Agbendeh, Z. M., Iorungwa, P. D., Surma, N. and Amua, Q. M. (2020) Synthesis, Characterization, Kinetics, Thermodynamics and Nematicidal studies of Sm(III), Gd(III) and Nd(III) Schiff base complexes. *ChemSearch Journal*, 11 (2), 24-34.

Iorungwa, M. S., Wuana,R. A., Dafa, S. T. (2019). Synthesis, Characterization, Kinetics,

Thermodynamic and Antimicrobial Studies of Fe(III), Cu(II), Zn(II), N,N'-Bis(2-hydroxy-1,2-diphenylethanone)ethylenediamine Complexes. *Chemical Methodologies***,** 3 (2), 408-424.

Jalal M., Hammouti B., R. Touzani, A. Aouniti, Ozdemir I. (2020), Metal-NHC heterocycle complexes in catalysis and biological applications: Systematic review, *Materials Today: Proceedings*, 31(S1), S122-S129, https://doi.org/10.1016/j.matpr.2020.06.398

Kapusterynska, A., Bijani, C., Palwoda, D., Vendier, L., Bourdon, V., Imbert, N., Cojean, S., Loiseau, P.M., Recchia, D., Scoffone, V. C., Degiacomi, G., Akhir, A., Saxena, D., Chopra, S., Lubenets, V. and Baltas, M. C. (2023) Mechanochemical studies on coupling of hydrazines and hydrazine amides with phenolic and furanyl aldehydes-hydrazones with antileishmanial and antibacterial activities. *Molecules*, 28(13), 5284. doi: 10.3390/molecules28135284

Khamaysa O.M.A., Selatnia I., Zeghache H., Lgaz H., Sid A., Chung I-M., Benahmed M., Gherraf N., Mosset P. (2020), Enhanced corrosion inhibition of carbon steel in HCl solution by a newly synthesized hydrazone derivative: Mechanism exploration from electrochemical, XPS, and computational studies, *Journal of Molecular Liquids*, 315, 113805, ISSN 0167-7322, https://doi.org/10.1016/j.molliq.2020.113805

Khan, Y., Sadia, H., Ali Shah, S. Z., Khan, M. N., Shah, A. A., *et al*. (2022) Classification, Synthetic, and Characterization Approaches to Nanoparticles, and Their Applications in Various Fields of Nanotechnology: A Review. *Catalysts*, 12(11), 1386. https://doi.org/10.3390/catal12111386

Kharissova, O. V., Kharisov, B. I., Gonzȧlez, C. M. O., Mendez, Y. P. and Lôpez, I. (2019) Greener synthesis of chemical compounds and materials. *Royal Society Open Science*, 6 (11), 191378.

Kitanosono T. and Kobayashi S., (2021). Synthetic organic "aquachemistry" that relies on neither cosolvents nor surfactants. *ACS Central Sciences*, 7 (5), 739-747.

Kostova I. (2023). The Role of Complexes of Biogenic Metals in Living Organisms. *Inorganics*, 11(2), 56. https://doi.org/10.3390/inorganics11020056

Kotynia, A., Wiatrak, B., Kamysz, W., Neubauer, D., Jawień, P.and Marciniak, A. (2021). Cationic Peptides and Their Cu(II) and Ni(II) Complexes: Coordination and Biological Characteristics. *International Journal of Molecular Sciences*, 22(21), 12028. https://doi.org/10.3390/ijms222112028

Liu, R., Cui, J., Ding, T., Liu, Y. and Liang, H. (2022) Research progress on the biological activities of metal complexes bearing polycyclic aromatic hydrazones. *Molecules*, 27 (23), 8393.

López-Lorent, Á. I., Pena-Pereira, F., Pedersen-Bjergaard, S., *et al*. (2022). The ten principles of green sample preparation. *TrAC Trends in Analytical Chemistry*, 148, 678-690.

Luo J., (2014) Electronic Properties and Oxidation/Reduction Chemistry of a Series of Late Transition Metal Complexes. Dissertations Submitted to Chemistry Department, Washington University in ST. Louis, Pp 36-60.

Mansour, M.S.A., Abdelkarim, A.T., El-Sherif, A.A. and Mahmoud, W. H. (2024) Metal complexes featuring a quinazoline schiff base ligand and glycine: synthesis, characterization, DFT and molecular docking analyses revealing their potent antibacterial, anti-helicobacter pylori, and anti-COVID-19 activities. *BMC Chemistry* 18, 150. https://doi.org/10.1186/s13065-024-01239-7

Martínez L., (2018). Measuring the conductivity of very dilute electrolyte solutions, drop by drop. *Journal Química Nova*, XY (1-4): 200-204. Http://dx.doi.org/10.21577/0100-4042.20170216.

Masand V.H., Mahajan D.T., Patil K.N., Hadda T.B., Youssoufi M.H., Jawarkar R.D., Shibi I.G. (2013) Optimization of antimalarial activity of synthetic prodiginines: QSAR, GUSAR, and CoMFA analyses. *Chem Biol Drug Des.* 81(4), 527-36. doi: 10.1111/cbdd.12099. PMID: 23279875

Munusamy, G. R., Appadurai, R. D., Kuppusamy S., Michael, P.G., Savarimuthu I. (2016) Ovicidal and larvicidal activities of some plant extracts against Aedes aegypti L. and Culex quinquefasciatus Say (Diptera: Culicidae). *Asian Pacific Journal of Tropical Disease*, 6 (6), 468-471.

Oladipo, H. J., Tajudeen, Y. A., Oladunjoye, I. O., Yusuff, S. I., *et al*. (2022) Increasing challenges of malaria control in sub-Saharan Africa: Priorities for public health research and policymakers. *Annals of Medicine and Surgery*, 81, 104366. https://doi.org/10.1016/j.amsu.2022.104366

Ommenya, F.K., Nyawade, D.M. and Kinyua, J. (2020) Synthesis, characterization and antibacterial activity of Schiffbase, 4-chloro-2-{(E)-[(4-flurophenyl)imino]methyl}phenol metal (II) complexes. *Journal of Chemistry*, 2020, 1-8.

Ong S. and Jaal Z., (2018) Larval age and nutrition affect the susceptibility of *Culex quinquefasciatus* (Diptera: Culicidae) to temephos. *Journal of Insect Science*, 18 (2), 38-46.

Pavčnik T., Radi M., Lužanin O., Dedryvère R., Tchitchekova D. S., Ponrouch A., Biten, J., Dominko R. (2024) Effect of ligand variation on Mg alkoxyborate electrolytes: Does more fluorine help? *Journal of Power Sources*, 626, 235711. https://doi.org/10.1016/j.jpowsour.2024.235711

Plowe C.V., (2022) Malaria chemoprevention and drug resistance: a review of the literature and policy implications. *Malaria Journal*, 21, 104. https://doi.org/10.1186/s12936-022-04115-8

Rai, R., Pandey, S., Rai, S.P. (2011) Arsenic-Induced Changes in Morphological, Physiological, and Biochemical Attributes and Artemisinin Biosynthesis in Artemisia Annua, an Antimalarial Plant. *Ecotoxicology*, 20, 1900–1913

Ramkumar, G., Karthi, S., Shivakumar, M. S. and Kweka, E. J. (2019) *Culex quinquefasciatus* Egg Membrane Alteration and Ovicidal Activity of Cipadessa baccifera (Roth) Plant Extracts Compared to Synthetic Insect Growth Regulators. *Research and Reports in Tropical Medicine*, 10, 145. https://doi.org/10.2147/RRTM.S227590

Ravindran, D. R., Bharathithasan, M., Ramaiah, P., Rasat, M. S. M., *et al*(2020). Chemical composition and larvicidal activity of flower extracts from *Clitoria ternatea* against *Aedes* (Diptera: Culicidae). *Journal of Chemistry*, 1155, 38372207.

Saleh H.M., Hassan A. I., (2023) Synthesis and characterization of nanomaterials for application in cost-effective electrochemical devices. *Sustainability*, 15 (14), 10891. https://doi.org/10.3390/su151410891

Santiago, P. H., Santiago, M. B., Martins, C. H. and Gatto, C. C. (2020) Copper(II) and zinc(II) complexes with Hydrazone: Synthesis, crystal structure, Hirshfeld surface and antibacterial activity. *Inorganica Chimica Acta*, 508, 119632

Sarıoğlu, A. O., Bulut, Z., Kahraman, T. D., *et al*. (2024) Homoleptic metal complexes derived from hydrazones as ligand; synthesis, cytotoxic activity, photoluminescence properties and ADMET studies. *Journal of Molecular Structure*, 1303, 137496. doi.org/10.1016/j.molstruc.2024.137496

Segovia, X., Srivastava, B., Serrato-Arroyo, S., Guerrero, A. and Huijben, S. (2025) Assessing fitness costs in malaria parasites: a comprehensive review and implications for drug resistance management. *Malaria Journal*, 24, 65. https://doi.org/10.1186/s12936-025-05286-w

Shakdofa, M. M. E., Shtaiwi, M. H., Morsy, N. and Abdel-rassel, T. A. (2014) Metal complexes of hydrazones and their biological, analytical and catalytic applications: A review. *Journal of Main Group Chemistry*, 13 (3), 187-218. DOI: 10.3233/MGC-140133

Sharma, D., Sharma, V., Sharma, A., Goyal, R., Tonk, R. K., Thakur, V.K. and Sharma, P.C. (2021). Green Chemistry approaches for thiazole containing compounds as a potential scaffold for cancer therapy. *Sustainable Chemistry and Pharmacy*, 23(21): 100496

Sharma, P. C., Sharma, D., Sharma, A., Saini, N, *et al*. (2020). Hydrazone comprising compounds as promising anti-infective agents: chemistry and structure-property relationship. Materials today Chemistry, 18, 100349. doi.org/10.1016/j.mtchem.2020.100349

Shinada, N. K., de Brevern, A. G. and Schimidtke, P. (2019) Halogen in protein bonding mechanism: Structural perspective. *Journal of Medicinal Chemistry*, 62 (21), 9341-9356; https://doi.org/10.1021/acs.jmedchem.8b01453

Sillo, A. J., Markirita, W. E., Swai, H. and Chancha, M. (2019) Larvicidal activity of *Hypoestes forskaolii* (Vahl) R. Br root extracts against *Anopheles gambiae* Giless.s, *Aedes aegypti* L, and *Culex quinquefasciatus Say*. *Journal of Experimental Pharmacology*, 11, 23-27.

Sirimula, S., Bailey, J., Vegesna, R. and Narayan, M. (2013). Halogen interactions in protein-ligand complexes: Implications of halogen bonding for rational drug design. *Journal of Chemical Information and Modeling*, 53 (11), 2781-2791; https://doi.org/10.1021/ci400257k

Sittel, T., Trumm, M., Adam, C. and Geist, A. (2021). Impact of solvent polarity on the ligand configuration in tetravalent thorium N-Donor complexes. *Inorganic Chemistry*, 60(2), 456.

Snaha, K., Narayanankutty, A., Job, J. T., Olatunj, O. J., Alfarhan, A., Famurewa, A. C. and Ramesh, V. (2022). Antimicrobial and Larvicidal Activities of Different Ocimum Essential Oils Extracted by Ultrasound-Assisted Hydrodistillation. *Molecules*, 27 (5), 1456.

Takken, W., Charlwood, D. and Lindsay, S.W. (2024) The behaviour of adult *Anopheles gambiae*, sub-Saharan Africa's principal malaria vector, and its relevance to malaria control: a review. *Malaria Journal*, 23, 161. https://doi.org/10.1186/s12936-024-04982-3

Titi A., Messali M., Warad I., Hiroshi O., Hammouti B., Touzani R. (2020a), Synthesis of novel $Cl_2Co_4L_6$ cluster using 1-hydroxymethyl-3,5-dimethylpyrazole (LH) ligand: Crystal structure, spectral, thermal, Hirschfeld surface analysis and catalytic oxidation evaluation, *Journal of Molecular Structure*, 1199, 126995; https://doi.org/10.1016/j.molstruc.2019.126995

Titi A., Warad I., Almutairi S.M., Fettouhi M., *et al*. (2020b), One-pot liquid microwave-assisted green synthesis of neutral trans-Cl2Cu(NNOH)2: XRD/HSA-interactions, antifungal and antibacterial evaluations, *Inorganic Chemistry Communications*, Volume 122, 2020, 108292, ISSN 1387-7003, https://doi.org/10.1016/j.inoche.2020.108292

Uddin, S., Hossain, M.S., Latif, M.A., Karin, M.R., Mohapatra, R.K. and Kudrat-E-Zahan, M. (2019). Antimicrobial activity of Mn complexes incorporating Schiff bases: A short review. *American Journal of Hetrocyclic Chemistry*, 5 (2), 27-36

Venkatesan, T., Choi, Y. W. and Kim, Y. K. (2019) Impact of Different Extraction Solvents on Phenolic Content and Antioxidant Potential of *Pinus densiflora* Bark Extract. Biochemistry Research International, 2019, 3520675. doi: 10.1155/2019/3520

Wang, Y., Cheng, P., Jiao, B., Song, X., Wang, H., Wang, H., Wang, H., Huang, X., Liu, H.and Gong, M. (2020) Investigation of mosquito larval habitats and insecticide resistance in an area with a high incidence of mosquito-borne diseases in Jining, Shandong Province. *PLoS ONE*, 15(3), e0229764. https://doi.org/10.1371/journal.pone.0229764

Wang, Y., Guo, S., Yu, L., Zhang, W., Wang, Z., Chi, Y. R. and Wu, J. (2024) Hydrazone derivatives in agrochemical discovery and development. Chinese Chemical Letters, 35 (3), 108207. https://doi.org/10.1016/j.cclet.2023.10820

White, N.J. (2019). Triple artemisinin-containing combination anti-malarial treatments should be implemented now to delay the emergence of resistance. *Malaria Journal*, 18, 338. https://doi.org/10.1186/s12936-019-2955-z

WHO (2024). Multiple first-line therapies as part of the response to antimalarial drug resistance. An implementation guides. https://www.who.int/publications/i/item/9789240103603

WHO interim position statement (2016). The role of larviciding for malaria control in sub-saharan Africa. Accessed 25 march, 2022.

Yang, X., Zhou, G., Sun, L. and Zheng, C. (2021) Ovicidal activity of spirotetramat and its effect on hatching, development and formation of Frankliniella occidentalis egg. *Scientific Reports*, 11, 20751. https://doi.org/10.1038/s41598-021-00160-6

Zanin, C. R. F., Trindade, F. T. T. and Silva, A. A. (2019) Effect of different food and sugar sources on the larval biology and adult longevity of *Anopheles darling* (Diptera: Culicidae). *Tropical Biomedicine*, 36 (2), 569-577.

Zou, X., Ji, L., Ge, J. and Sadoway, D. R. (2019) Electrodeposition of crystalline silicon films from silicon dioxide for low-cost photovoltaic applications. *Nature Communications*, 10 (1), 5772.